Electronic Supplementary Information (ESI)

Thermodynamic properties of selenoether-functionalized ionic liquids and their use for the synthesis zinc selenide nanoparticles

Karsten Klauke,[a] Dzmitry H. Zaitsau,[b] Mark Bülow,[c] Li He,[a] Maximilian Klopotowski,[a] Tim-Oliver Knedel,[a] Juri Barthel,[d] Christoph Held,*[c] Sergey P. Verevkin*[b] and Christoph Janiak*[a]

a   Institut für Anorganische Chemie und Strukturchemie, Heinrich-Heine-Universität Düsseldorf, Universitätsstraße 1, D-40225 Düsseldorf,Germany

b   Department of Physical Chemistry, Universität Rostock, Dr.-Lorenz-Weg 2 ,D-18059 Rostock, Germany

c   Department BCI, Laboratory of Thermodynamics, Technische Universität Dortmund, Emil-Figge-Str. 70, D-44227 Dortmund

d   Gemeinschaftslabor für Elektronenmikroskopie RWTH-Aachen, Ernst-Ruska-Centrum für Mikroskopie und Spektroskopie mit Elektronen, D-52425, Jülich, Germany

E-mail adresses:

Karsten Klauke: Karsten.Klauke@hhu.de
Dr. Dzmitry H. Zaitsau: zaitsaudz@gmail.com
Mark Bülow: mark.buelow@tu-dortmund.de
Li He: hli88dafa@googlemail.com
Maximilian Klopotowski: Maximilian.Klopotowski@uni-duesseldorf.de
Tim-Oliver Knedel: Tim-Oliver.Knedel@uni-duesseldorf.de
Dr. Juri Barthel: Ju.Barthel@fz-juelich.de
Dr. Christoph Held: Christoph.Held@tu-dortmund.de
Prof. Dr. Sergey P. Verevkin: sergey.verevkin@uni-rostock.de
Prof. Dr. Christoph Janiak: janiak@uni-duesseldorf.de

I   Ionic Liquid synthesis

Ion chromatography

The purity of the obtained bis(trifluoromethane)solfonylimides was verified by ion chromatography (Dionex ICS-1100, with IonPac® AS22, 4 × 250 mm column). Only minor impurities of chloride, bromide and fluoride were detected, yielding an anion purity of >99% for each IL.
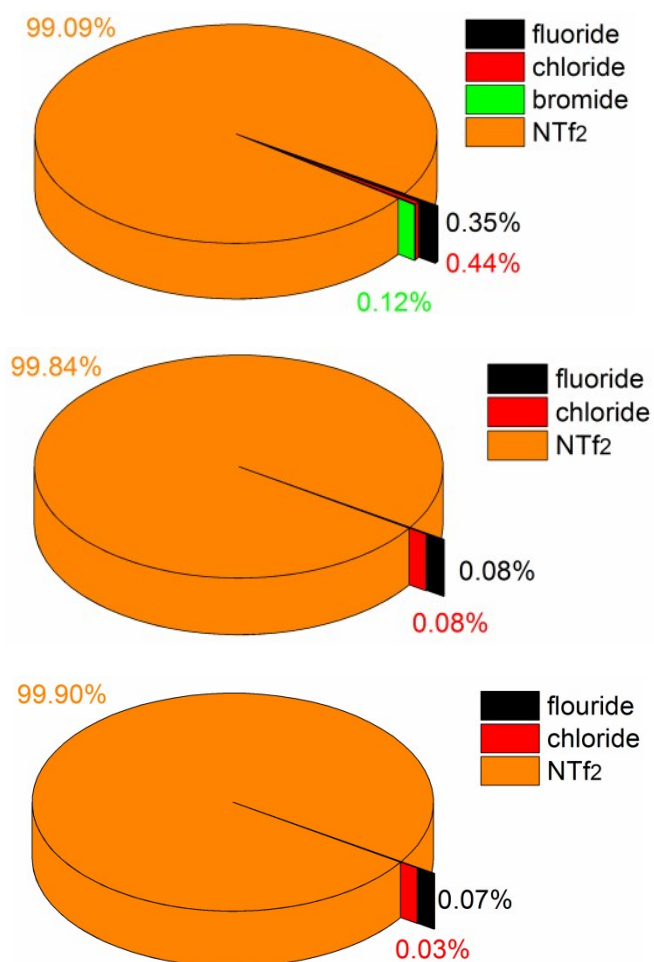

Figure S1. Results of the anion purity analysis by ion chromatography of **1-NTf$_2$** (top), **2-NTf$_2$** (middle) and **3-NTf$_2$** (below).

Table S1. Results of the anion purity analysis by ion chromatography of **1-, 2-** and **3-NTf$_2$** (measured and theoretical amount of [NTf$_2$]-anion)

IL	measured amount of NTf$_2^-$ [mg/L]	theoretical amount of NTf$_2^-$ [mg/L]
1-NTf$_2$	31 ± 1	35
2-NTf$_2$	44 ± 2	44
3-NTf$_2$	46 ± 1	45

NMR-spectra

***N*-[(phenylseleno)methylene]pyridinium bromide (1-Br)**
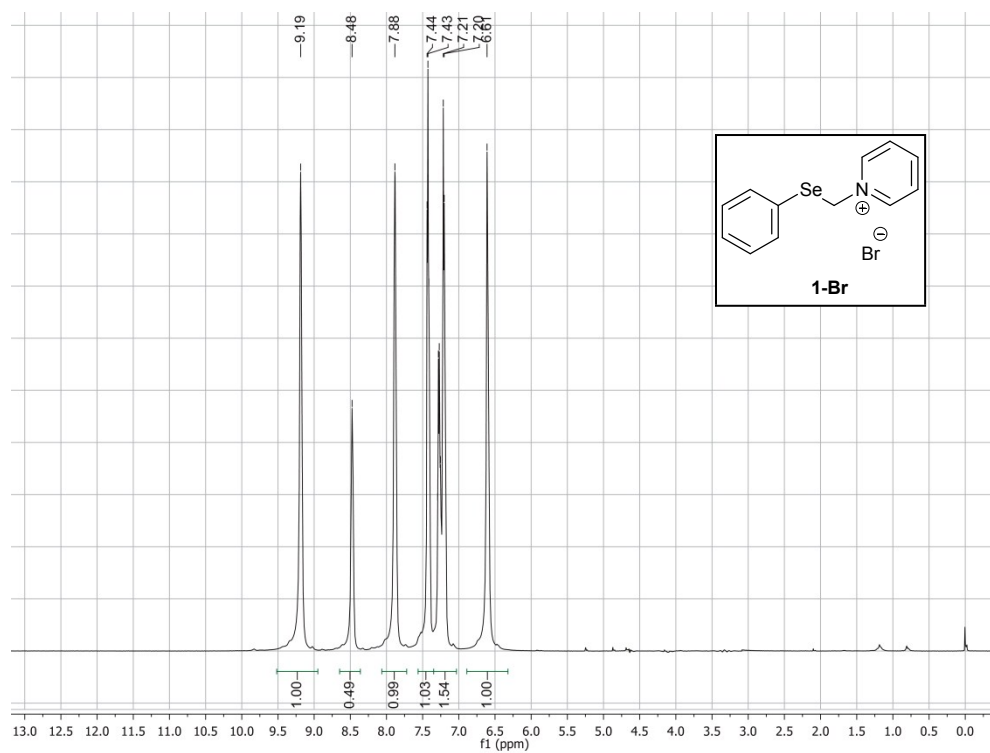

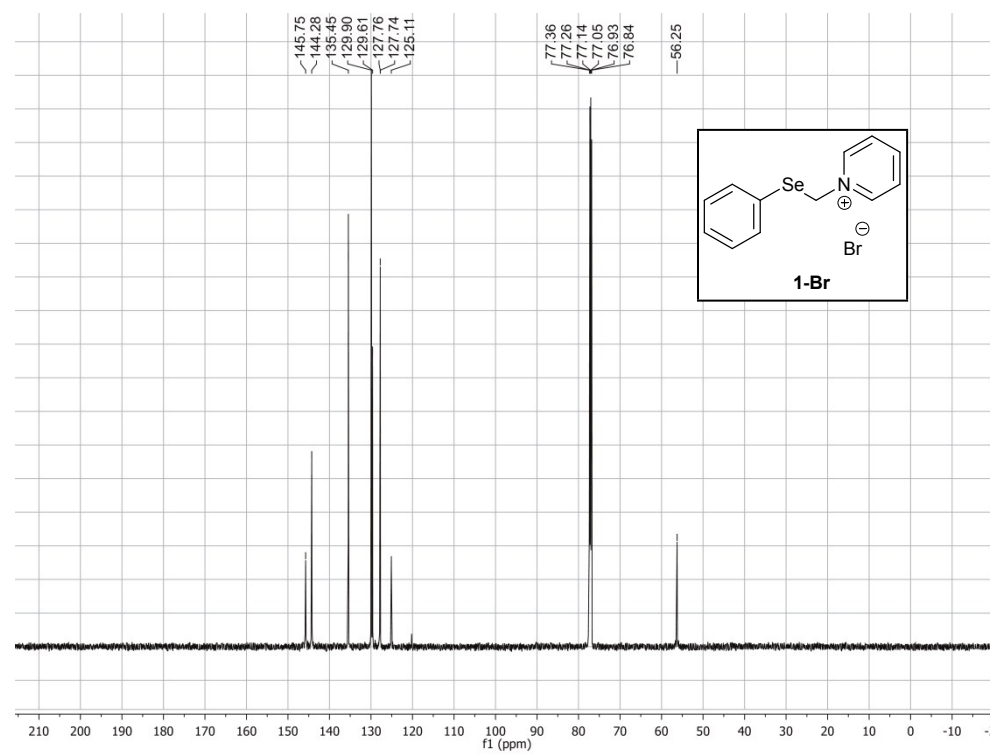**Figure S2.** 1-H-NMR-spectrum of compound **1-Br** in CDCl₃.

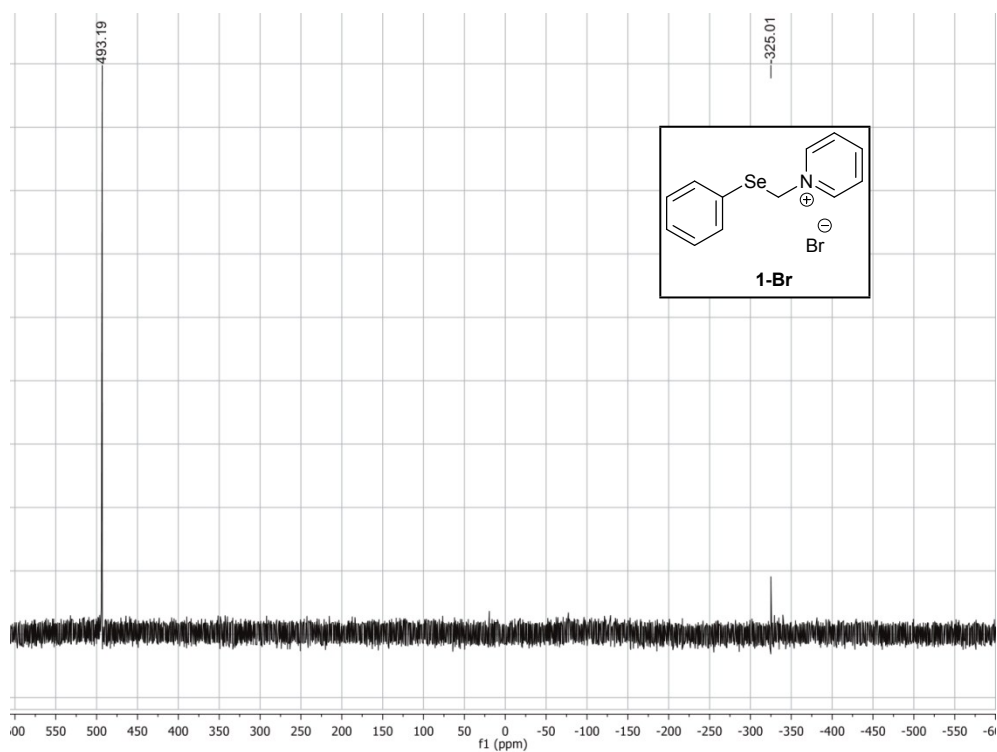**Figure S3.** ¹³C-NMR-spectrum of compound **1-Br** in CDCl₃.

Figure S4. ^{77}Se-NMR-spectrum of compound **1-Br** in CDCl$_3$.

N-methyl-N'-[(Phenylseleno)methylene)]imidazolium chloride (2-Cl)
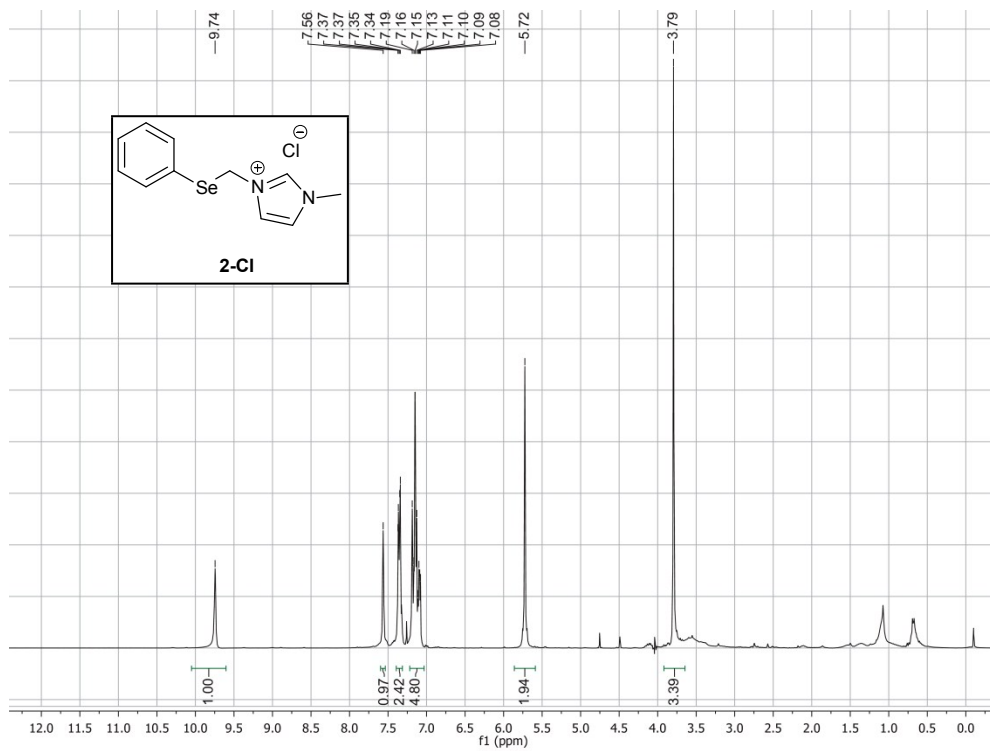
Figure S5. ^{1}H-NMR-spectrum of compound **2-Cl** in CDCl$_3$.
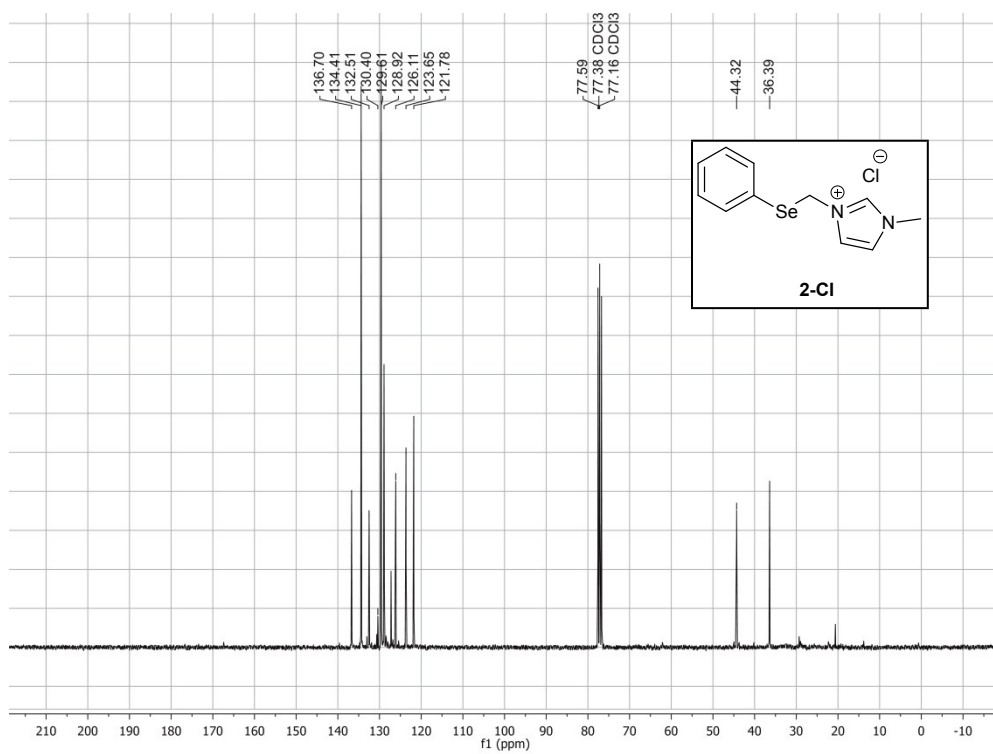
Figure S6. ^{13}C-NMR-spectrum of compound **2-Cl** in $CDCl_3$.
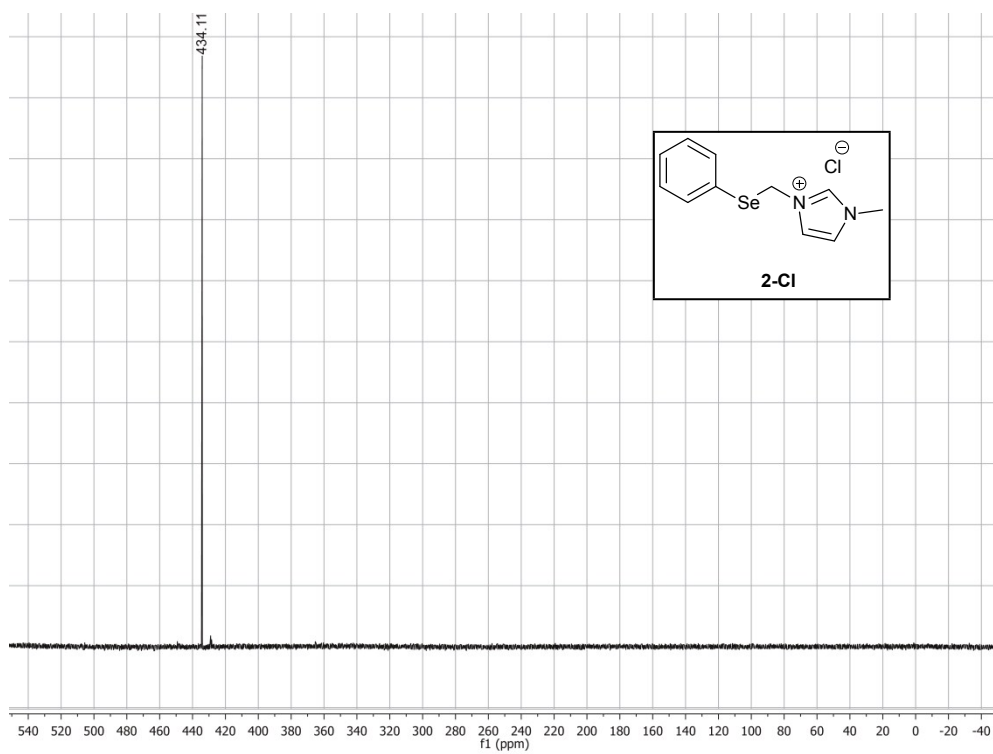
Figure S7. ^{77}Se-NMR-spectrum of compound **2-Cl** in $CDCl_3$.

N-butyl-N'-[(Phenylseleno)methylene)]imidazolium bromide (3-Br)
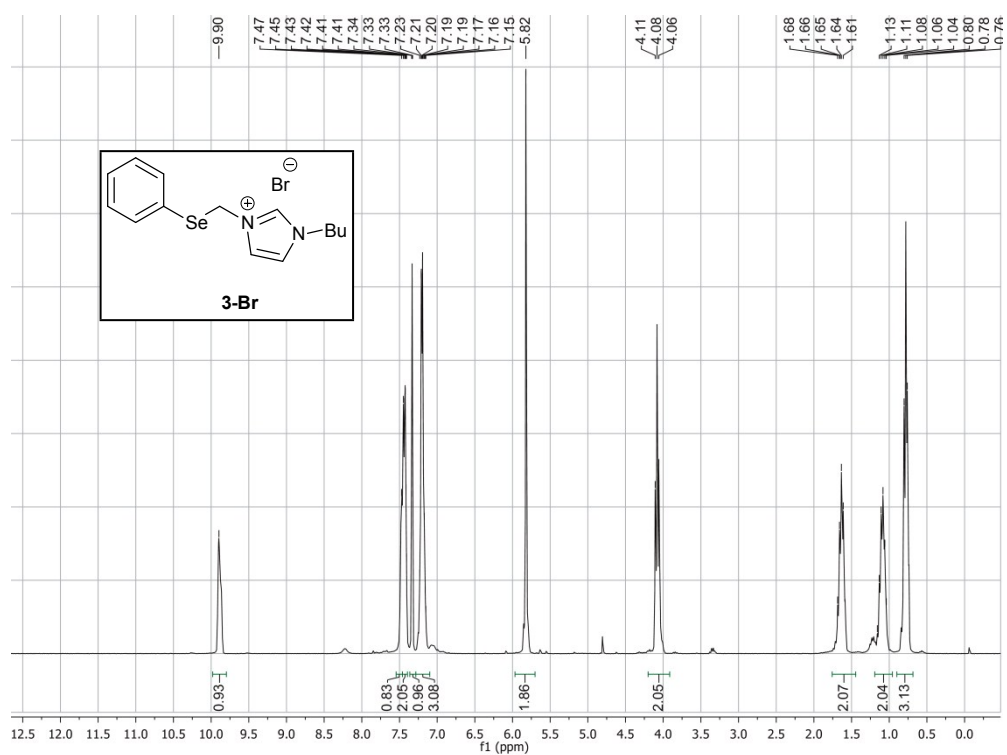
Figure S8. ^{1}H-NMR-spectrum of compound **3-Br** in CDCl$_3$.
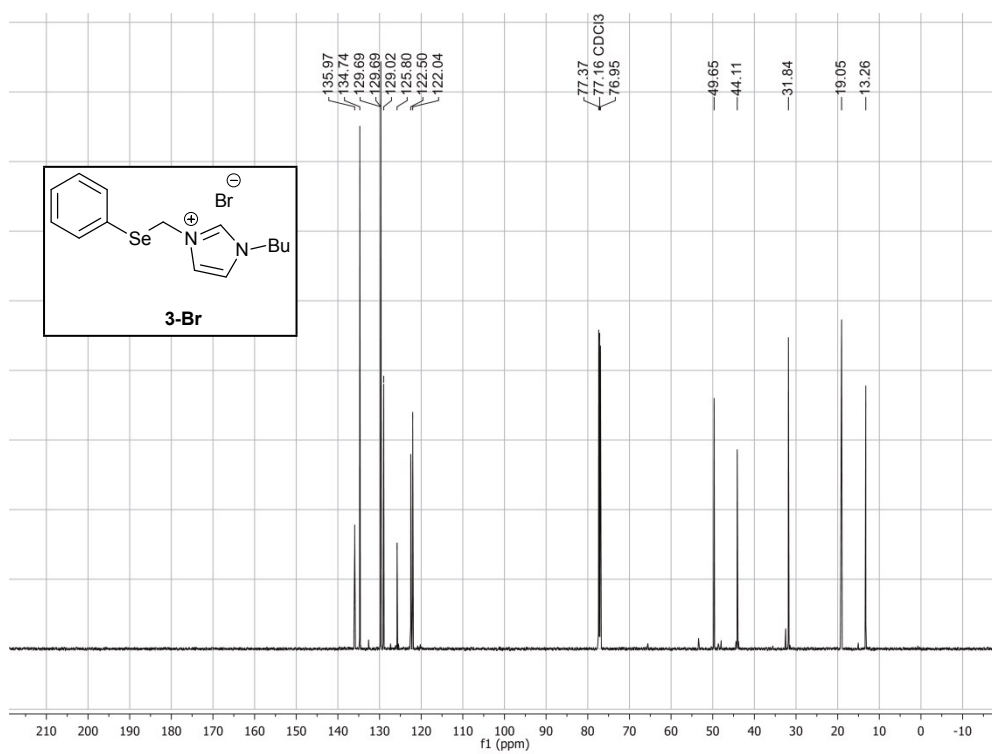
Figure S9. ^{13}C-NMR-spectrum of compound **3-Br** in CDCl$_3$.
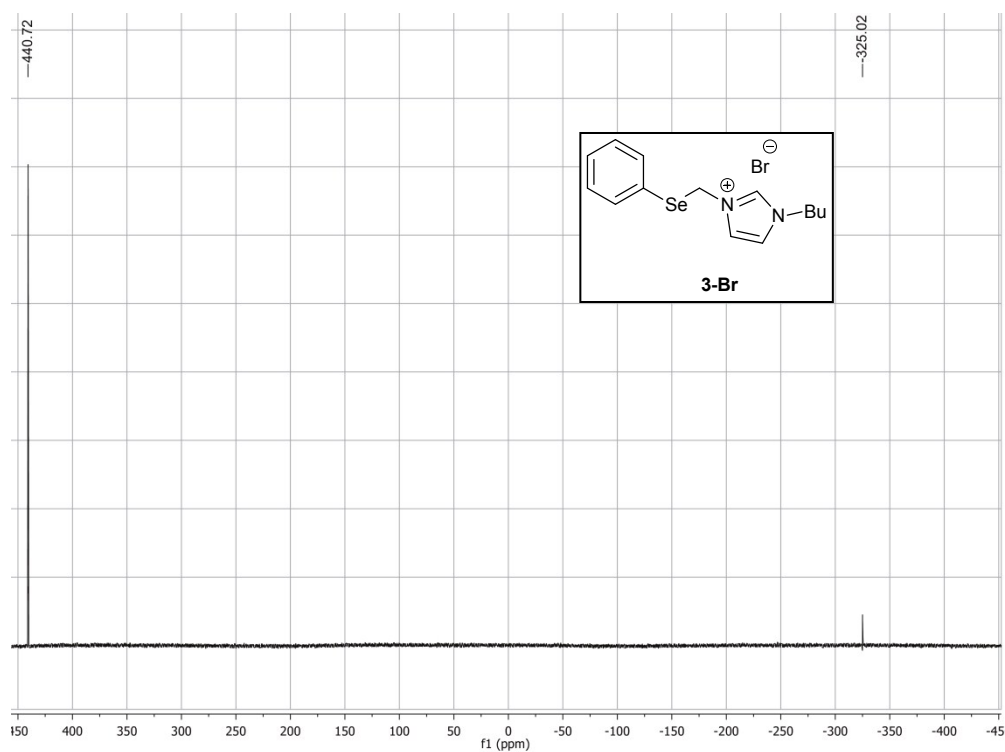
Figure S10. ^{77}Se-NMR-spectrum of compound **3-Br** in CDCl$_3$.

N-[(phenylseleno)methylene]pyridinium bis(trifluoromethanesulfonyl)imide (1-NTf$_2$)
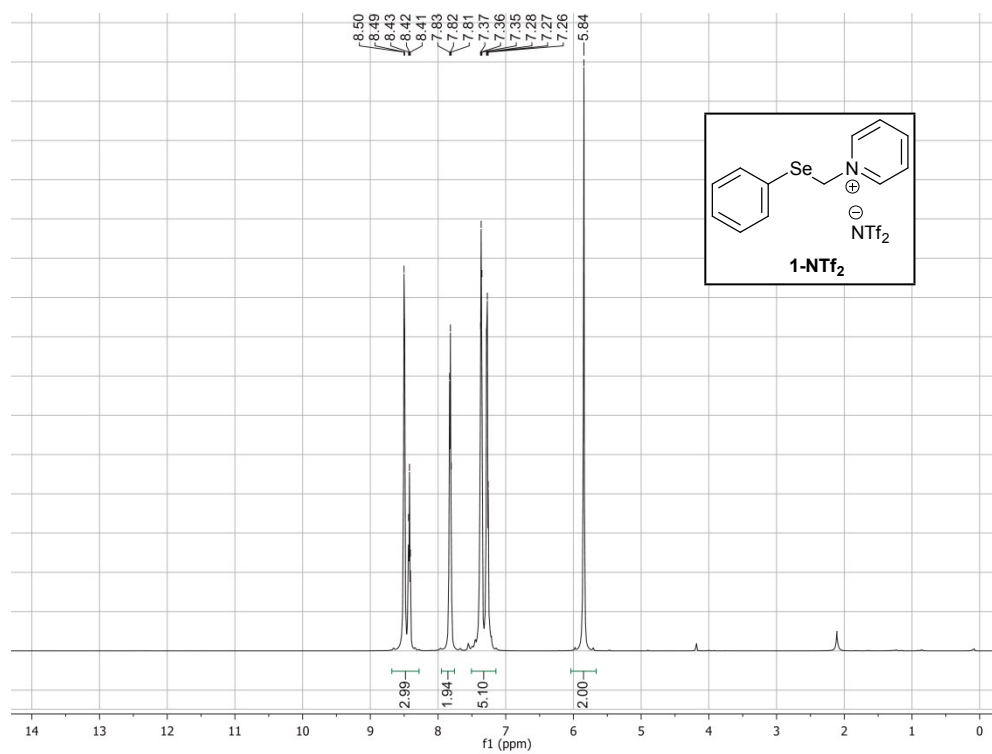
Figure S11. ^{1}H-NMR-spectrum of compound **1-NTf$_2$** in CDCl$_3$.
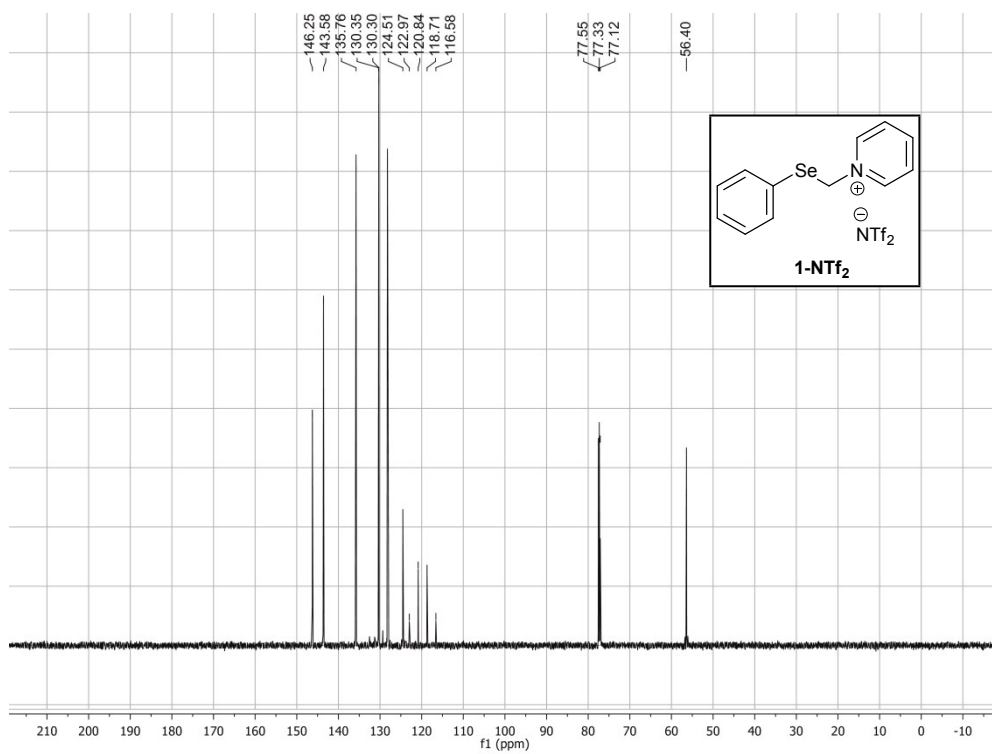
Figure S12. ^{13}C-NMR-spectrum of compound **1-NTf$_2$** in CDCl$_3$.
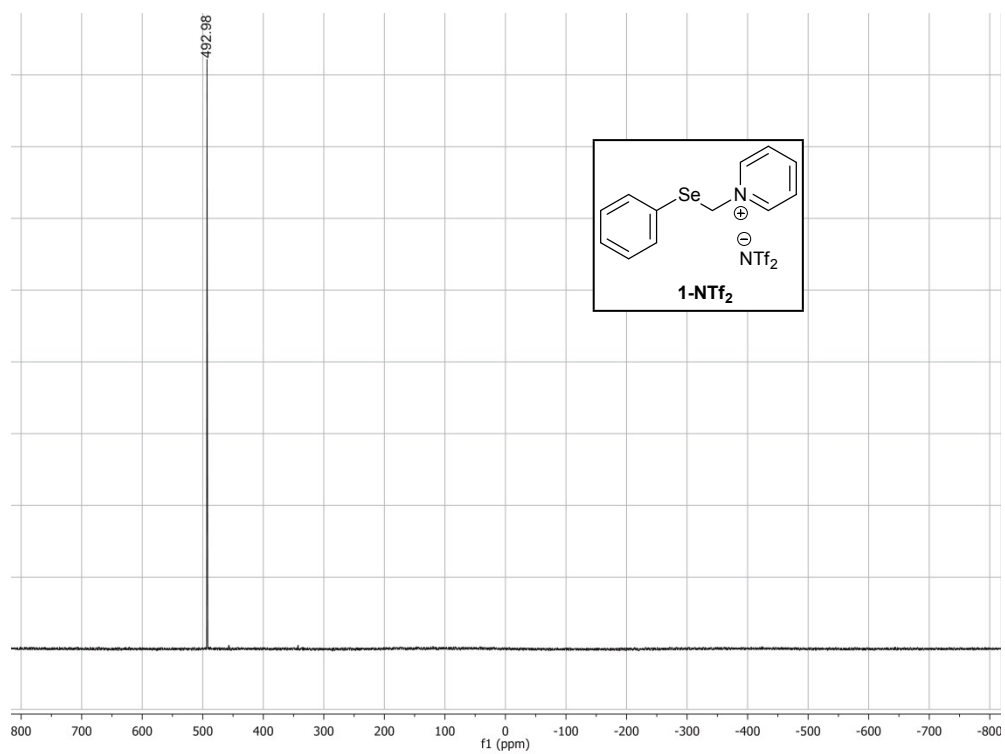
Figure S13. ^{77}Se-NMR-spectrum of compound **1-NTf$_2$** in CDCl$_3$.

_N_-methyl-_N'_-[(Phenylseleno)methylene)]imidazolium bis(trifluoromethanesulfonyl)imide (2-NTf₂)
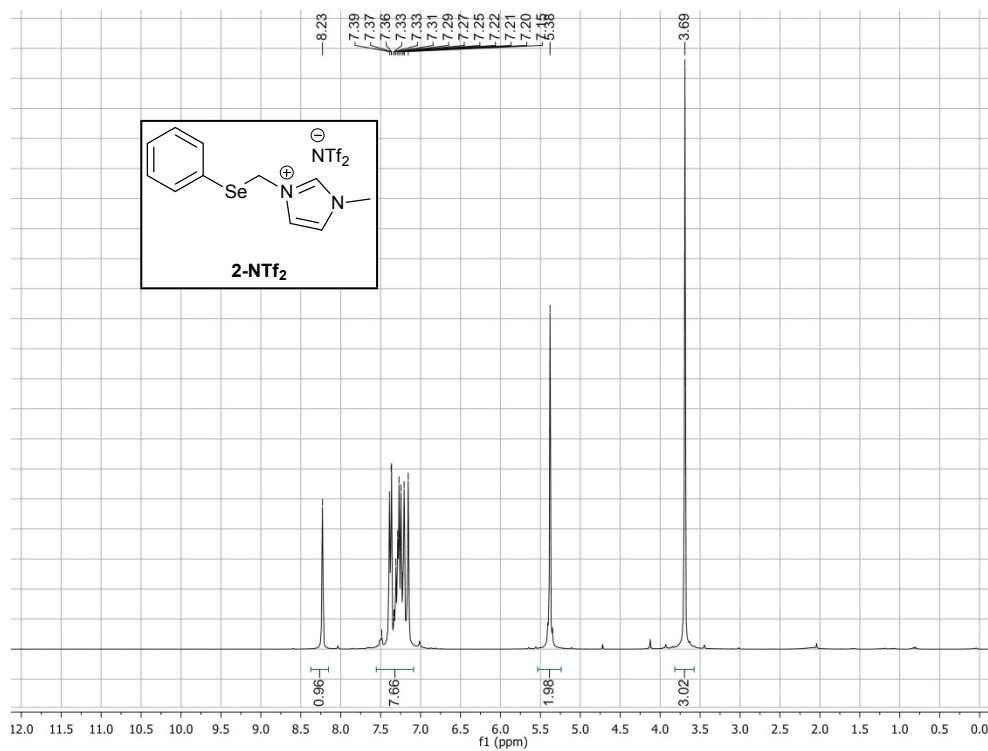
Figure S14. ¹H-NMR-spectrum of compound **2-NTf₂** in CDCl₃.
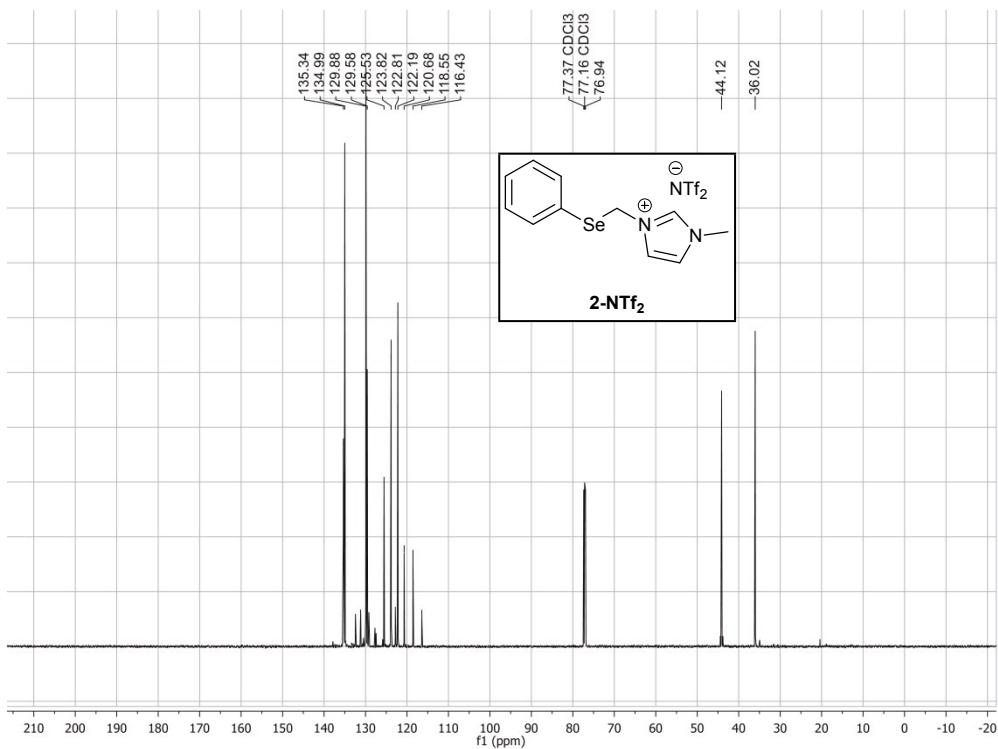
Figure S15. ¹³C-NMR-spectrum of compound **2-NTf₂** in CDCl₃.
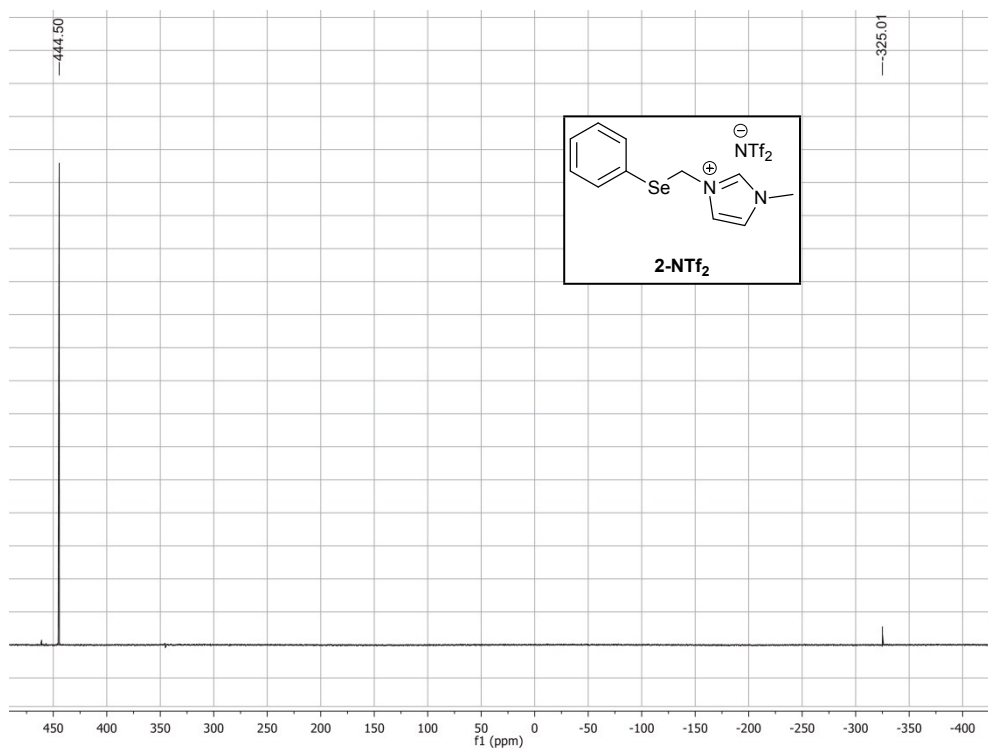
Figure S16. ^{77}Se-NMR-spectrum of compound **2-NTf$_2$** in CDCl$_3$.

***N*-butyl-*N'*-[(Phenylseleno)methylene)]imidazolium bis(trifluoromethanesulfonyl)imide (3-NTf$_2$)**
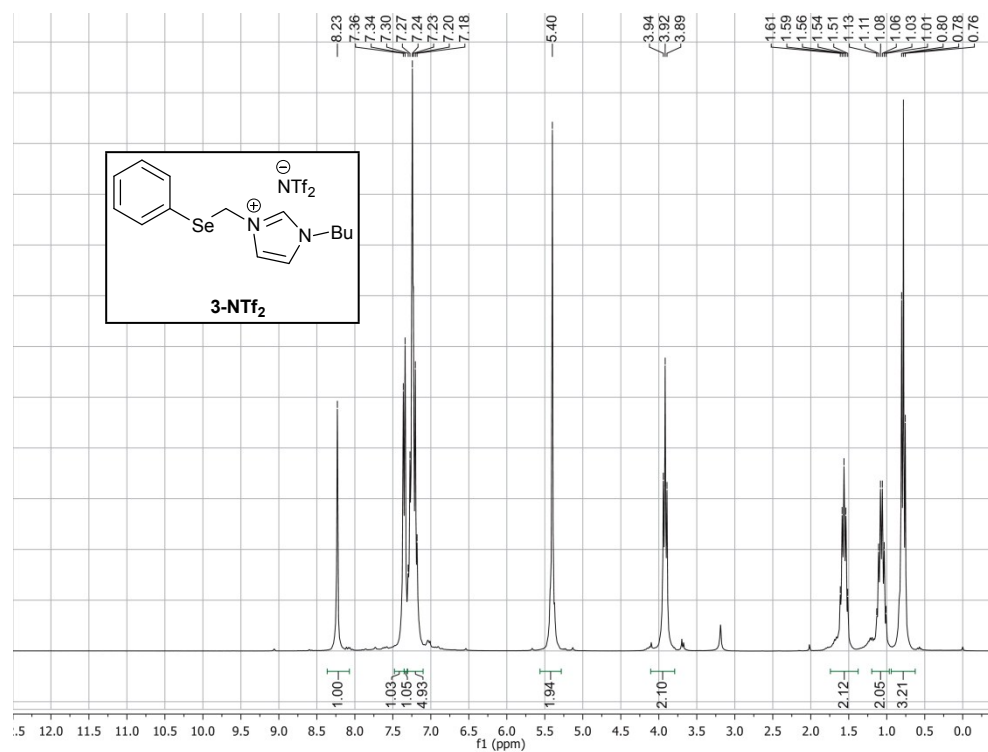
Figure S17. ^{1}H-NMR-spectrum of compound **3-NTf$_2$** in CDCl$_3$.
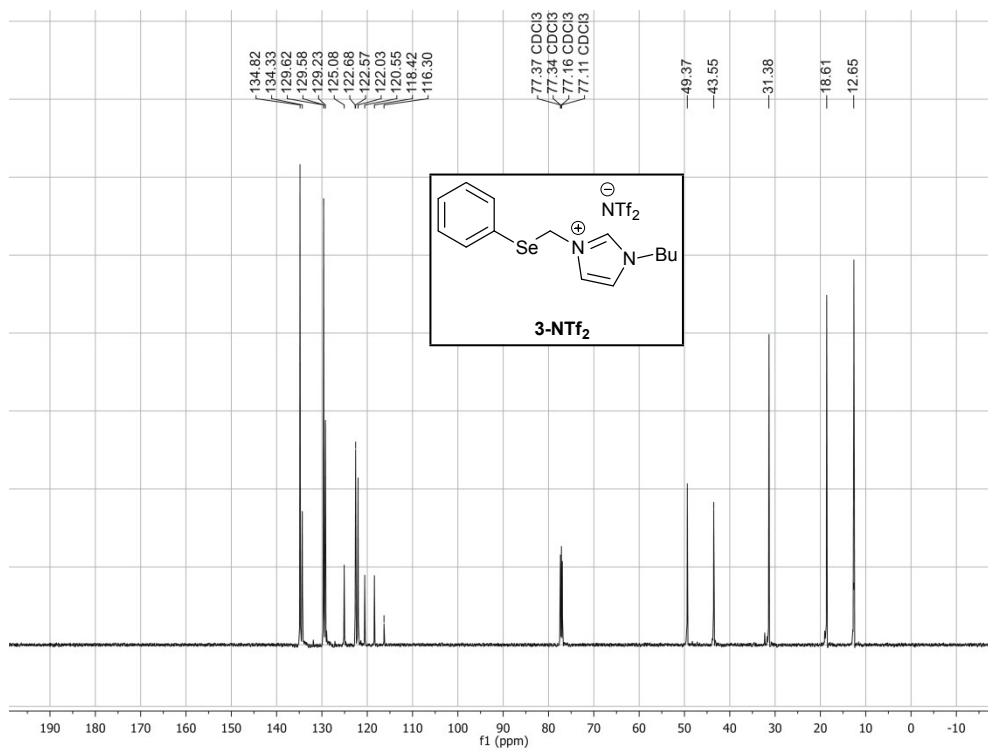
Figure S18. ^{13}C-NMR-spectrum of compound **3-NTf₂** in CDCl₃.
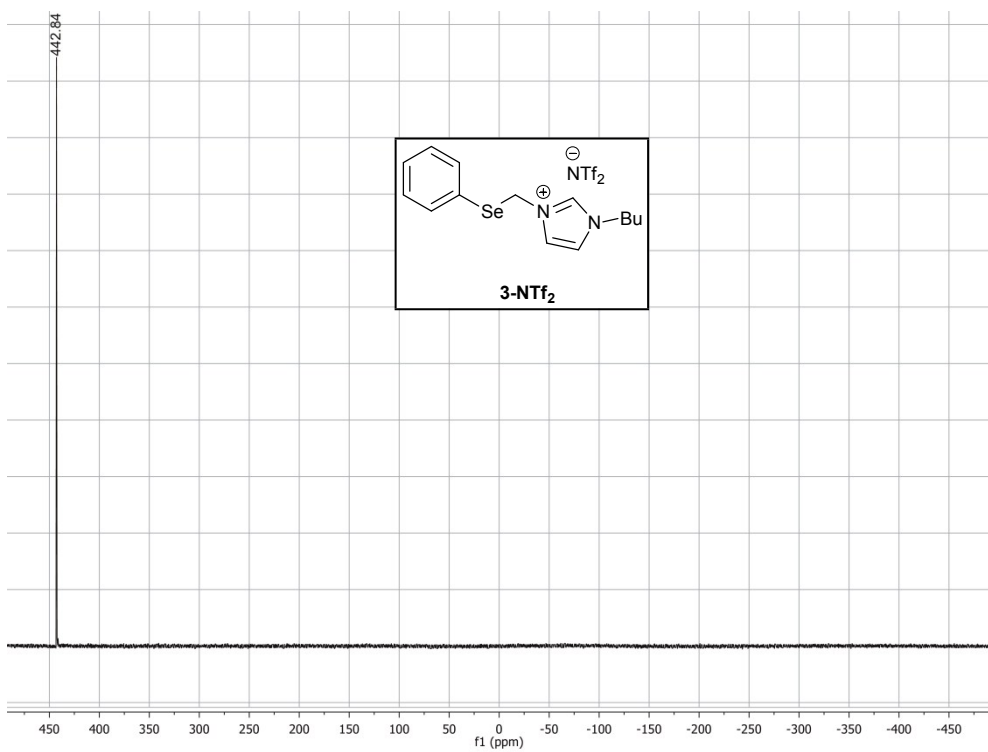
Figure S19. ^{77}Se-NMR-spectrum of compound **3-NTf₂** in CDCl₃.

N-methyl-*N'*-[(Phenylseleno)methylene)]imidazolium tetraphenylborate (2-BPh₄)
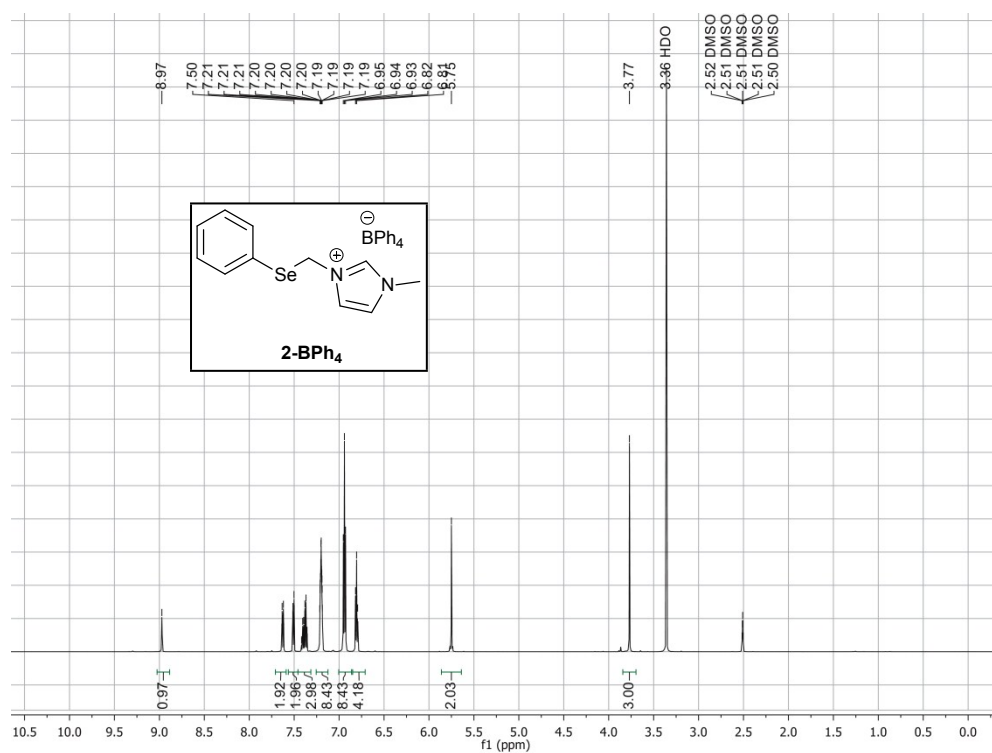
Figure S20. ¹H-NMR-spectrum of compound **2-BPh₄** in DMSO-d6.
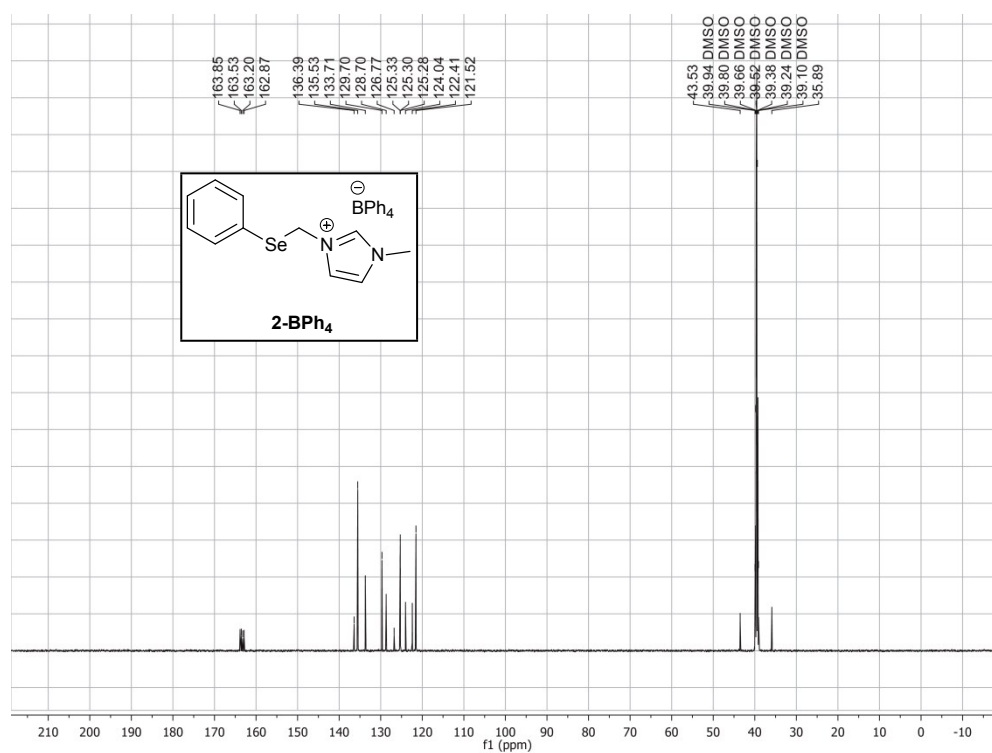
Figure S21. ¹³C-NMR-spectrum of compound **2-BPh₄** in DMSO-d6.
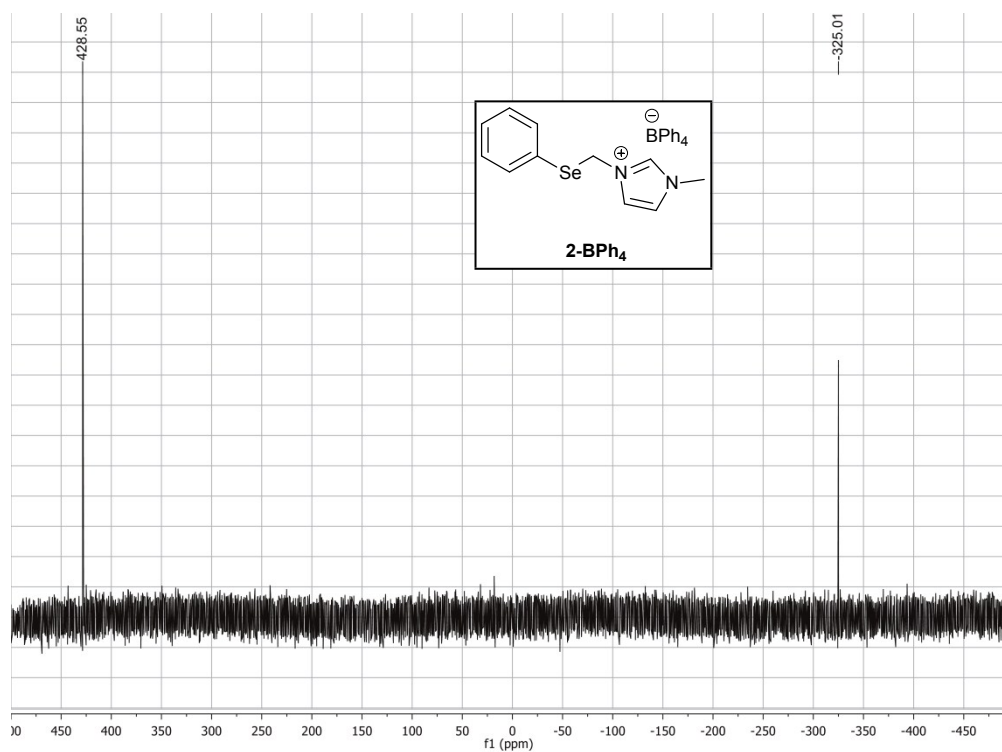
Figure S22. ^{77}Se-NMR-spectrum of compound **2-BPh$_4$** in DMSO-d6.

_N_-butyl-_N'_-[(Phenylseleno)methylene)]imidazolium tetraphenylborate (3-BPh$_4$)
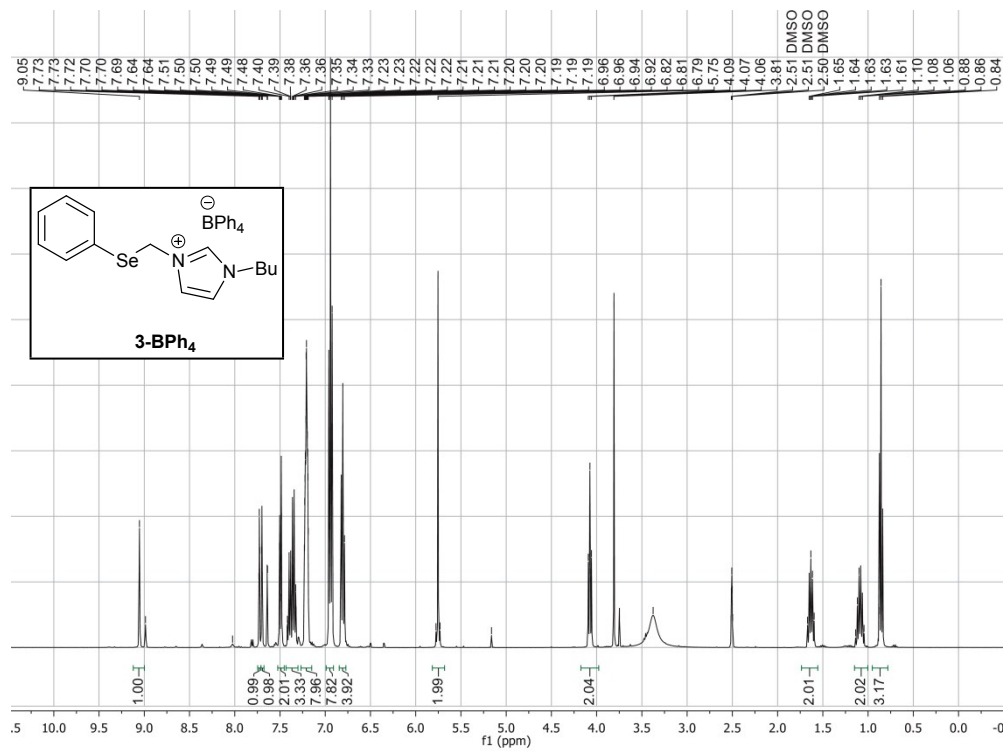
Figure S23. ^{1}H-NMR-spectrum of compound **3-BPh$_4$** in DMSO-d6.
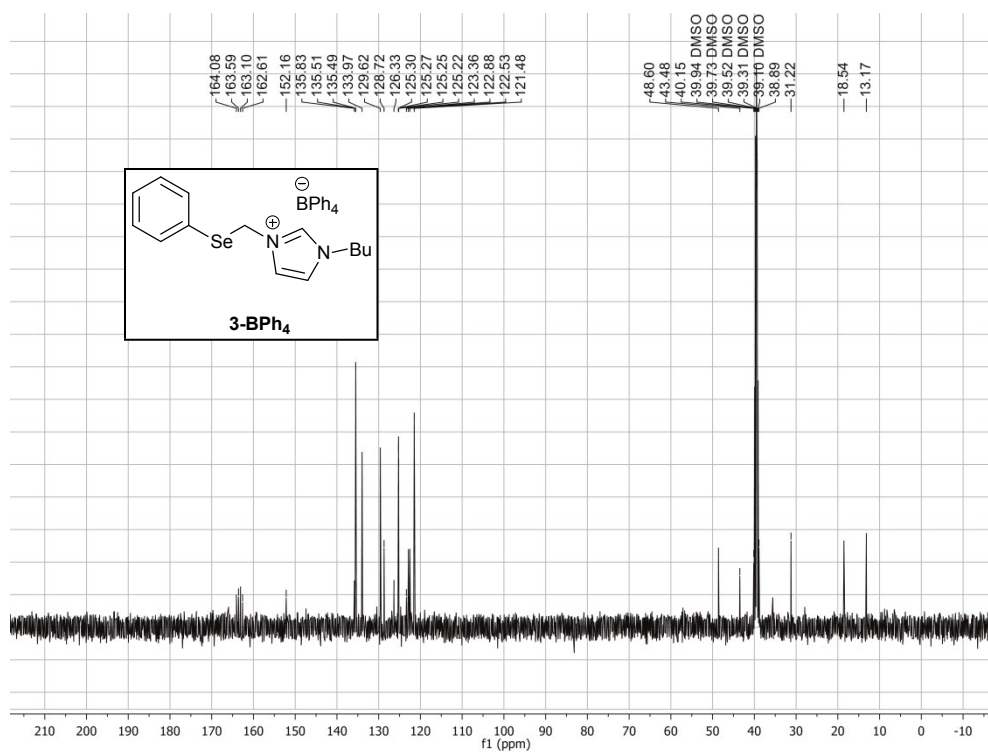
Figure S24. ^{13}C-NMR-spectrum of compound **3-BPh$_4$** in DMSO-d6.
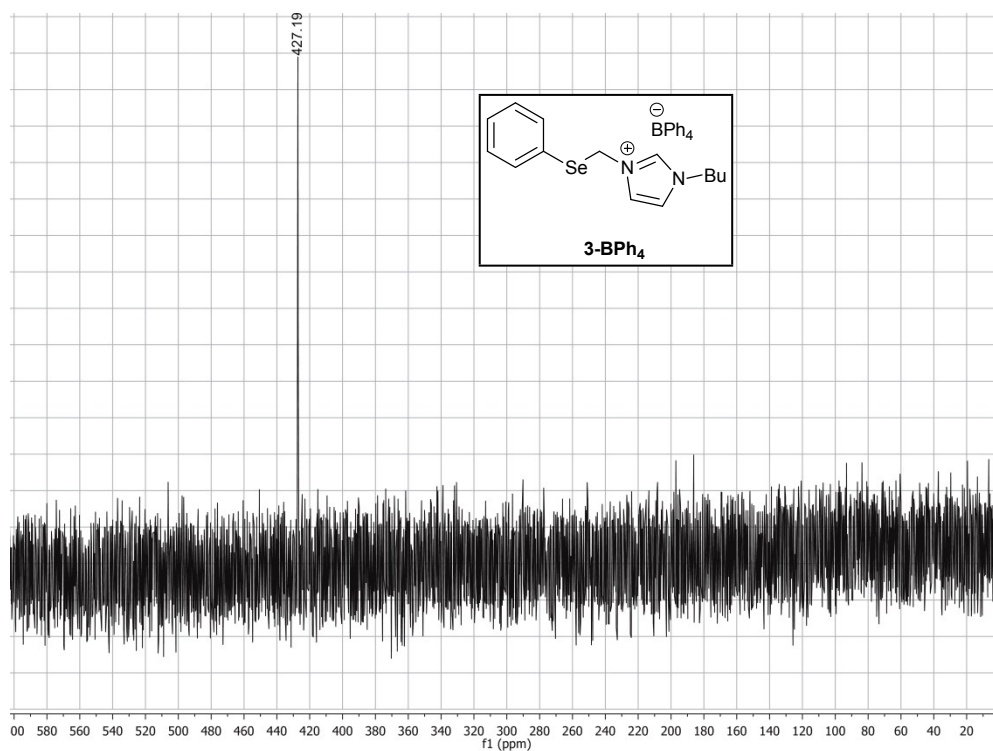
Figure S25. ^{77}Se-NMR-spectrum of compound **3-BPh$_4$** in DMSO-d6.

14

ESI-MS (Only the spectra of cations are shown)
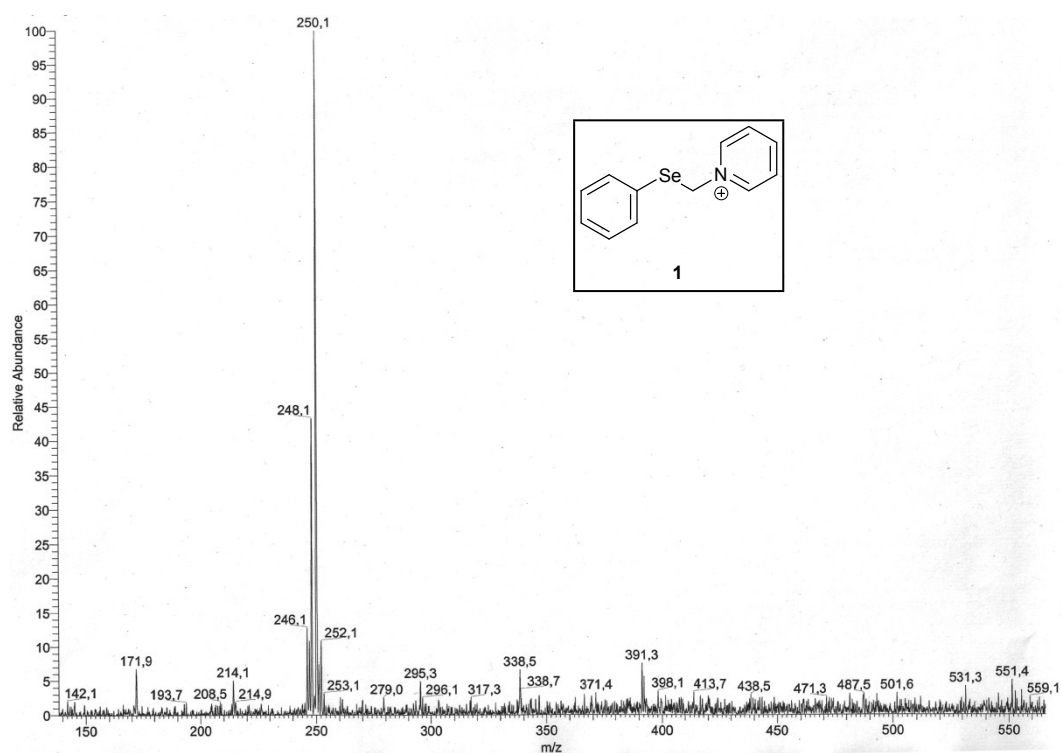
Figure S26. ESI-MS of the *N*-[(phenylseleno)methylene]pyridinium cation.
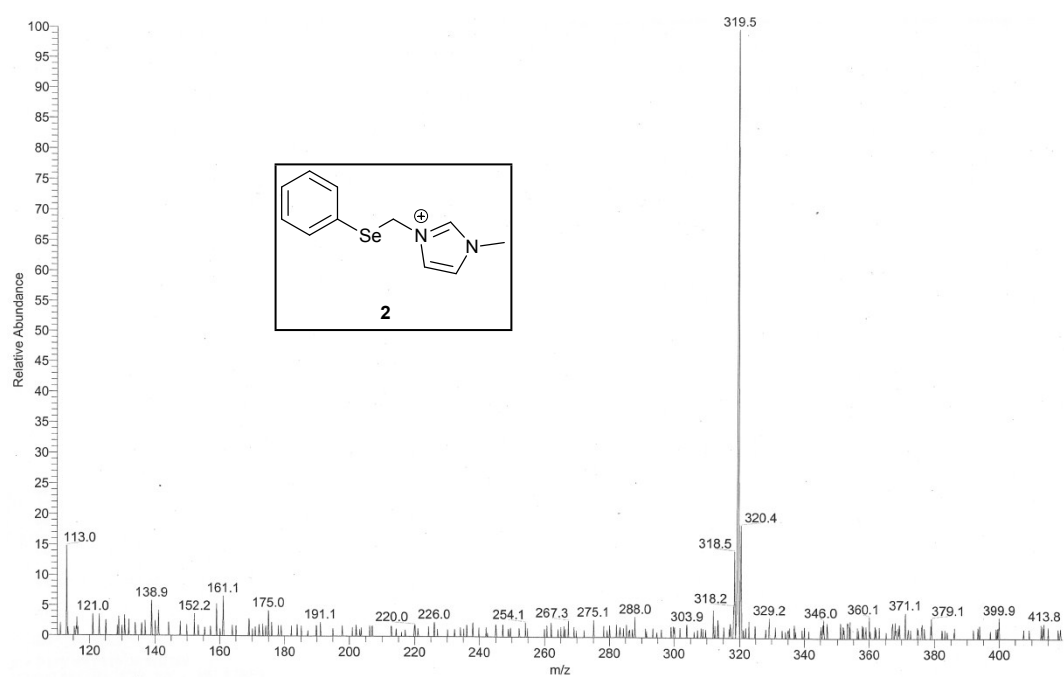
Figure S27. ESI-MS of the *N*-methyl-*N'*-[(Phenylseleno)methylene)]imidazolium cation.
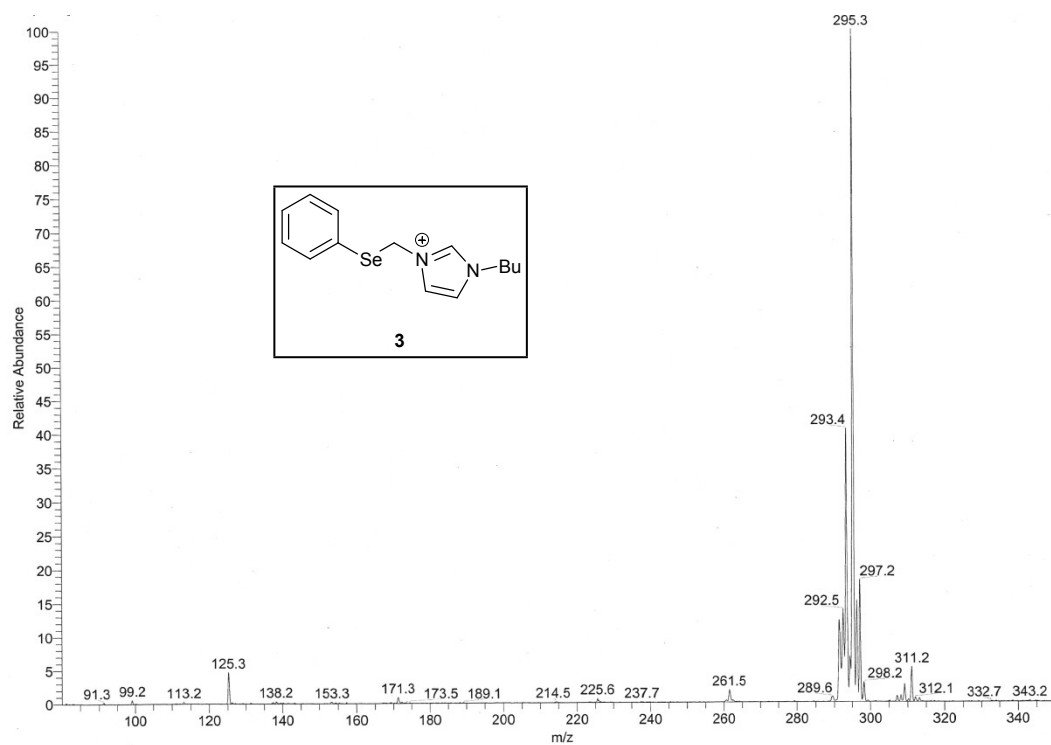
Figure S28. ESI-MS of the *N*-butyl-*N'*-[(Phenylseleno)methylene)]imidazolium cation.
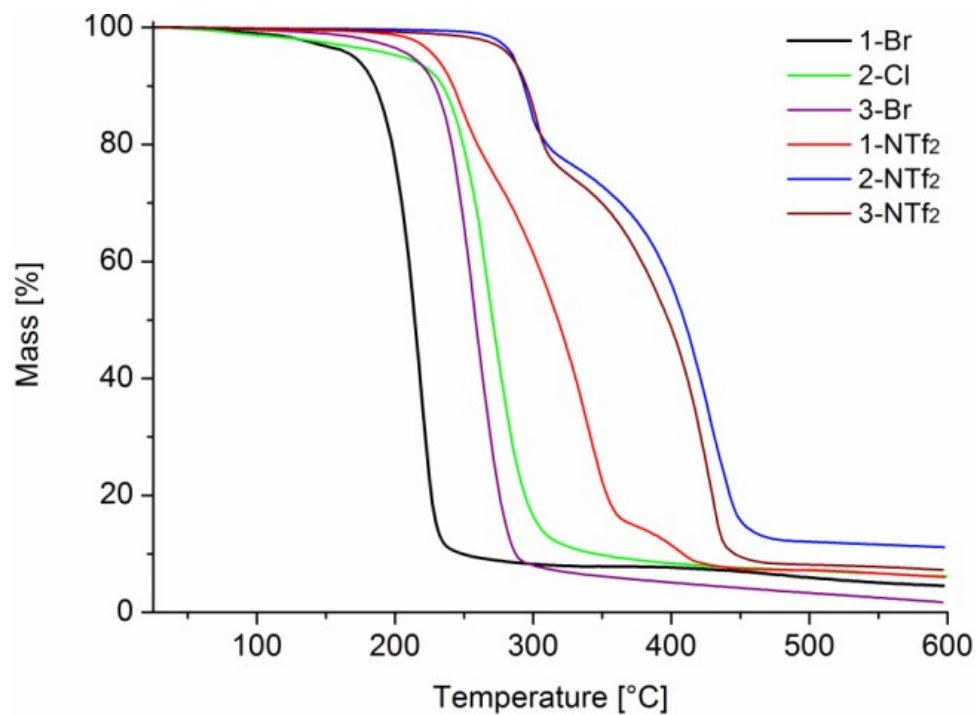
Figure S29. Thermogravimetric analysis of the selenoether-functionalized ionic liquids.

X-ray crystallography

Table S2. Crystallographic data and data refinement of compounds **1-Br**, **2-BPh$_4$** and **3-BPh$_4$**.

Compound	1-Br	2-BPh$_4$	3-BPh$_4$
CCDC-No.	1589574	1589576	1589575
Empirical formula	C$_{12}$H$_{12}$NSeBr	C$_{24}$H$_{20}$B·C$_{11}$H$_{13}$N$_2$Se	C$_{24}$H$_{20}$B·C$_{14}$H$_{19}$N$_2$Se
M [g·mol-1]	329.10	571.40	613.48
Crystal size [mm^3]	0.01 × 0.01 × 0.01	0.04 × 0.04 × 0.03	0.20 × 0.20 × 0.10
T (K)	140	140	140
Θ [°] (completeness)	2.33–27.53 (99.5 %)	2.18–24.96 (99.2 %)	2.31–22.13 (97.1 %)
h, k, l range	-10, 9, ±17, ±15	±15, ±29, ±30	±11, ±46, ±20
Crystal system	monoclinic	monoclinic	monoclinic
Space group	P2$_1$/n	P2$_1$	P2$_1$/n
a [Å]	7.8322 (4)	11.7606 (7)	9.8147 (10)
b [Å]	13.3857 (7)	30.594 (2)	38.702 (4)
c [Å]	11.6240 (6)	15.8656 (10)	17.1287 (18)
α [°]	90	90	90
β [°]	96.186 (2)	90.937 (3)	95.247 (5)
γ [°]	90	90	90
V [Å^3]	1211.56 (11)	5707.6 (6)	6479.0 (12)
Z	4	8	8
D$_{calc}$ [g·cm^{-3})]	1.804	1.330	1.258
μ (Mo Kα) [mm^{-1}]	6.364	1.343	1.187
F(000)	640	2368	2560
Max./min. transmission	0.7456/ 0.6862	1.0000/ 0.9118	1.0000/ 0.8909
Reflections collected	28271	91307	86945
Independent reflections	2810	25946	11922
(R$_{int}$)	(0.0328)	(0.0696)	(0.0973)
Data/ restraints/ parameters	2810/ 0/ 136	25946/ 1/ 1409	11922/ 25/ 759
Max./min. Δρ (e· Å^{-3})[a]	0.345/ -0.549	0.389/-0.546	1.350/-0.716
R$_1$/wR$_2$ [I>2σ (I)] [b]	0.0195/ 0.0450	0.0462/ 0.0839	0.0486/ 0.1128
R$_1$/wR$_2$ (all data)[b]	0.0245/ 0.0435	0.0875/ 0.0745	0.0912/ 0.1004
Goodness-of-fit (GOF) on F^2 [c]	1.045	0.952	1.058

[a] Largest difference peak and hole; [b] R$_1$ = [Σ(||Fo| − |Fc||)/Σ |Fo|]; wR$_2$ = [Σ [w(Fo^2 − Fc^2)^2]/Σ [w(Fo^2)^2]]$^{1/2}$; [c] Goodness-of-fit = [Σ [w(Fo^2 − Fc^2)^2]/(n–p)]$^{1/2}$; [d] Absolute structure parameter.[1]

Analysis of for possible π-stacking and C-H-π interactions

Significant π-stacking show rather short centroid-centroid contacts (<3.8 Å), near parallel ring planes (alpha < 10° to ~0° or even exactly 0° by symmetry), small slip angles (β, γ <25°) and vertical displacements (slippage <1.5 Å) which translate into a sizable overlap of the aryl-plane areas.[2,3]

Significant intermolecular C-H··· π contacts start around 2.7 Å for the (C)-H···ring centroid distances with H-perp also starting at below 2.6 – 2.7 Å and C-H··Cg > 145°.[2]
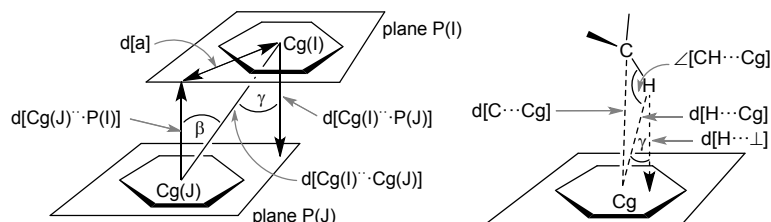
Scheme S1. Graphical presentation of the parameters used for the description of π···π stacking (left).[2] Graphical presentation of the parameters used for the description of CH- π interactions (right)[2]

Supramolecular packing analysis

In addition, the supramolecular packing analyses in the N-[(phenylseleno)methylene]pyridinium bromide salt (**1-Br**), the N-(methyl)-N'-[(phenylseleno)methylene]imidazolium tetraphenylborate (**2-BPh₄**) and N-(butyl)-N'-[(phenylseleno)methylene]imidazolium tetraphenylborate salt (**3-BPh₄**) were carried out by a quantitative analysis of non-covalent intermolecular interactions with Hirshfeld surfaces using the program CrystalExplorer[4] following the methodology outlined in ref.[5]

.

_N_-[(phenylseleno)methylene]pyridinium bromide 1-Br
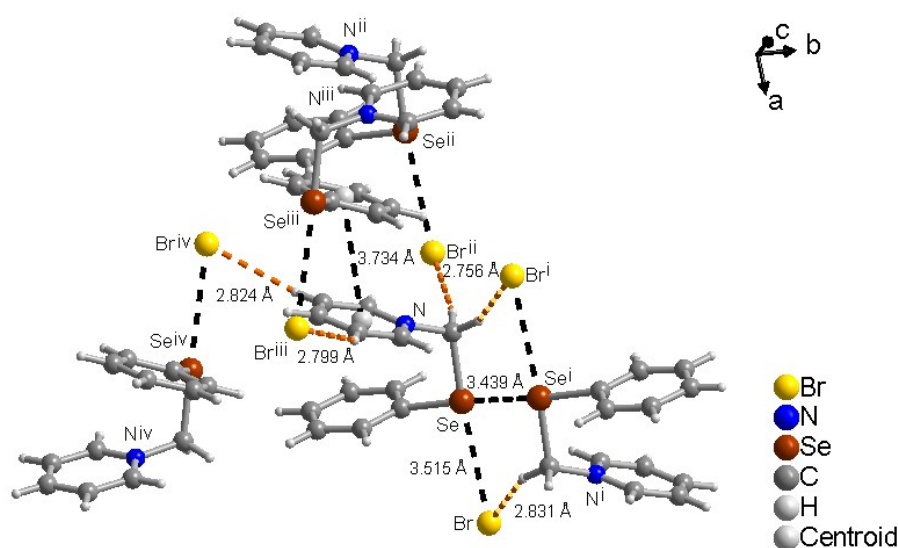
Figure S30: Section of the packing diagram of compound **1-Br** showing several intermolecular interactions like π-stacking along a-direction as well as Se–Se interactions (black dashed lines) and short C-H···Br distances (orange dashed lines). (i = i = -1/2+x,1/2-y,1/2+z, ii = 1/2-x,1/2+y,1/2-z, iii = 1-x,-y,1-z, iv = -1+x,y,z)

Table S3. Analysis of Short Ring-Interactions with Cg-Cg Distances <   6.0 Ang., Alpha < 20.000 Deg. and Beta < 60.0 Deg.

- Cg(I)   = Plane number I (= ring number in () above)
- Alpha   = Dihedral Angle between Planes I and J (Deg)
- Beta   = Angle Cg(I)-->Cg(J) or Cg(I)-->Me vector and normal to plane I (Deg)
- Gamma   = Angle Cg(I)-->Cg(J) vector and normal to plane J (Deg)
- Cg-Cg   = Distance between ring Centroids (Ang.)
- CgI_Perp = Perpendicular distance of Cg(I) on ring J (Ang.)
- CgJ_Perp = Perpendicular distance of Cg(J) on ring I (Ang.)
- Slippage = Distance between Cg(I) and Perpendicular Projection of Cg(J) on Ring I (Ang).

Cg(I)	Res(I)	Cg(J)	[ARU(J)]	Cg-Cg	Alpha	Beta	Gamma	CgI_Perp	CgJ_Perp	Slippage
Cg(1)	[1] -> Cg(2)	[1555.01]	4.0884(2)	27	38.5	33.1	-3.4252	3.2013	
Cg(1)	[1] -> Cg(2)	[4455.01]	3.7334(2)	6	22.8	27.7	3.3069	-3.4425	
Cg(1)	[1] -> Cg(2)	[4555.01]	5.3557(3)	6	59.5	55.4	-3.0416	2.7210	
Cg(2)	[1] -> Cg(1)	[1555.01]	4.0884(2)	27	33.1	38.5	3.2013	-3.4252	
Cg(2)	[1] -> Cg(1)	[4454.01]	5.3557(3)	6	55.4	59.5	2.7210	-3.0416	
Cg(2)	[1] -> Cg(1)	[4554.01]	3.7334(2)	6	27.7	22.8	-3.4425	3.3069	
			Min or Max	3.733	6.2	22.8	59.5	-3.442	-3.442	

[1555] = X,Y,Z
[4455] = -1/2+X,1/2-Y,1/2+Z
[4555] = 1/2+X,1/2-Y,1/2+Z
[4454] = -1/2+X,1/2-Y,-1/2+Z
[4554] = 1/2+X,1/2-Y,-1/2+Z
(Significant contacts are highlighted in yellow – reciprocal contacts are not highlighted)

Cg(1) = N–C(2)–C(4)–C(6)–C(5)–C(3)
Cg(2) = C(7)–C(8)–C(10)–C(12)–C(11)–C(9)

Table S4. Hydrogen-bond geometry [Å, º] of compound **1-Br**.

D-H···A	D—H	H···A	D···A	D—H···A
C(1)-H(1A)···Br[i]	0.99	2.83	3.7295(2)	151
C(1)-H(1B)···Br[ii]	0.99	2.76	3.7249(2)	166
C(4)-H(4)···Br[iii]	0.95	2.80	3.6106(2)	144
C(5)-H(5)···Br[iv]	0.95	2.82	3.7213(2)	158

i = -1/2+x,1/2-y,1/2+z
ii = 1/2-x,1/2+y,1/2-z
iii = 1-x,-y,1-z
iv = -1+x,y,z

The Hirshfeld surface (d_{norm}) of PhSeCH$_2$pyr$^+$ Br$^-$, **1-Br** displays close intermolecular contacts: around bromide and selenium ad from the CH$_2$ hydrogen atoms (red spots on the d_{norm} surface) (Figure S31). The majority of the surface is colored blue (representing the sum of longer than van-der-Waals contact distances). The relative contributions to the Hirshfeld surface area due to close intermolecular contacts are summarized in Table S5.

(a)   (b)
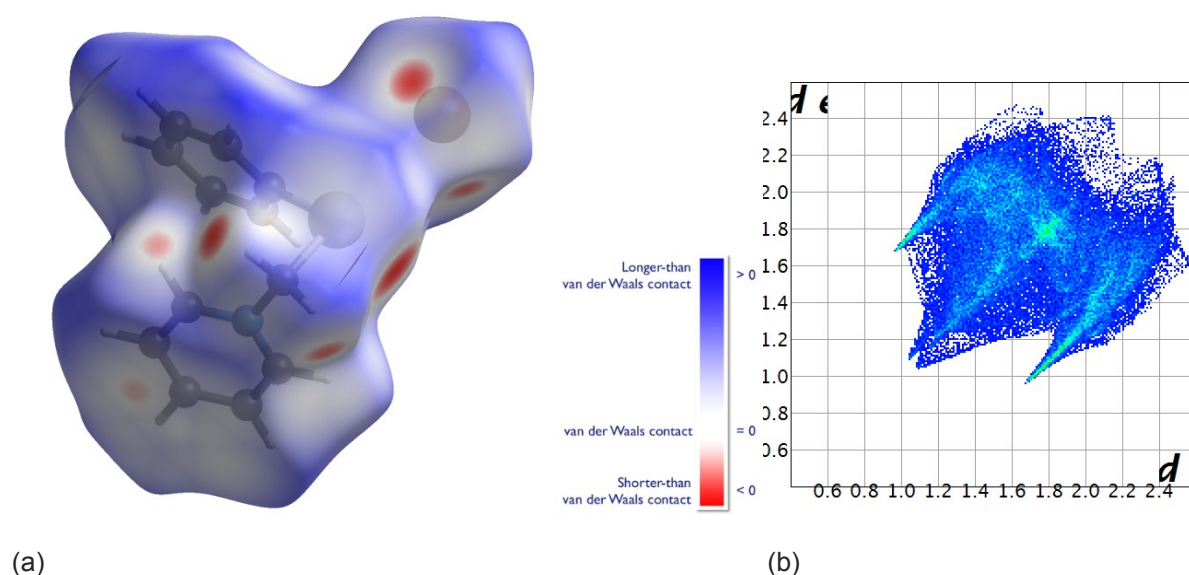
Figure S31. (a) Hirshfeld surface of **1-Br** mapped with the d_{norm} property.[5c] Red represents the closest contacts, and blue the most distant contacts.
(b) 2D fingerprint plot of **1-Br**. d_i (abscissa) and d_e (ordinate) are the distances from the surface to the nearest atom interior and exterior to the surface, respectively. For a breakdown of the fingerprint plot into the contributions from Br···H, Se···Se, C···H, H···H close intermolecular contacts (see Table S5 and Figure S32and S33).

Table S5. Percent contributions of close supramolecular interactions to Hirshfeld surface in **1-Br**.[a]

Interaction	Percent (%)	Figure
Br···H [a]	26.7	Figure 32(a)
Se···H [a]	7.5	
Se···Se [a]	0.7	Figure 33(b)
C···C (i.e. π···π) [a]	4.7	Figure 32(c)
C···H (i.e. C–H···π) [a]	10.3	Figure 33(a)
H···H [a]	46.7	Figure 33(b)
Sum	96.6	

[a] includes reciprocal contacts.

(a)

(b)
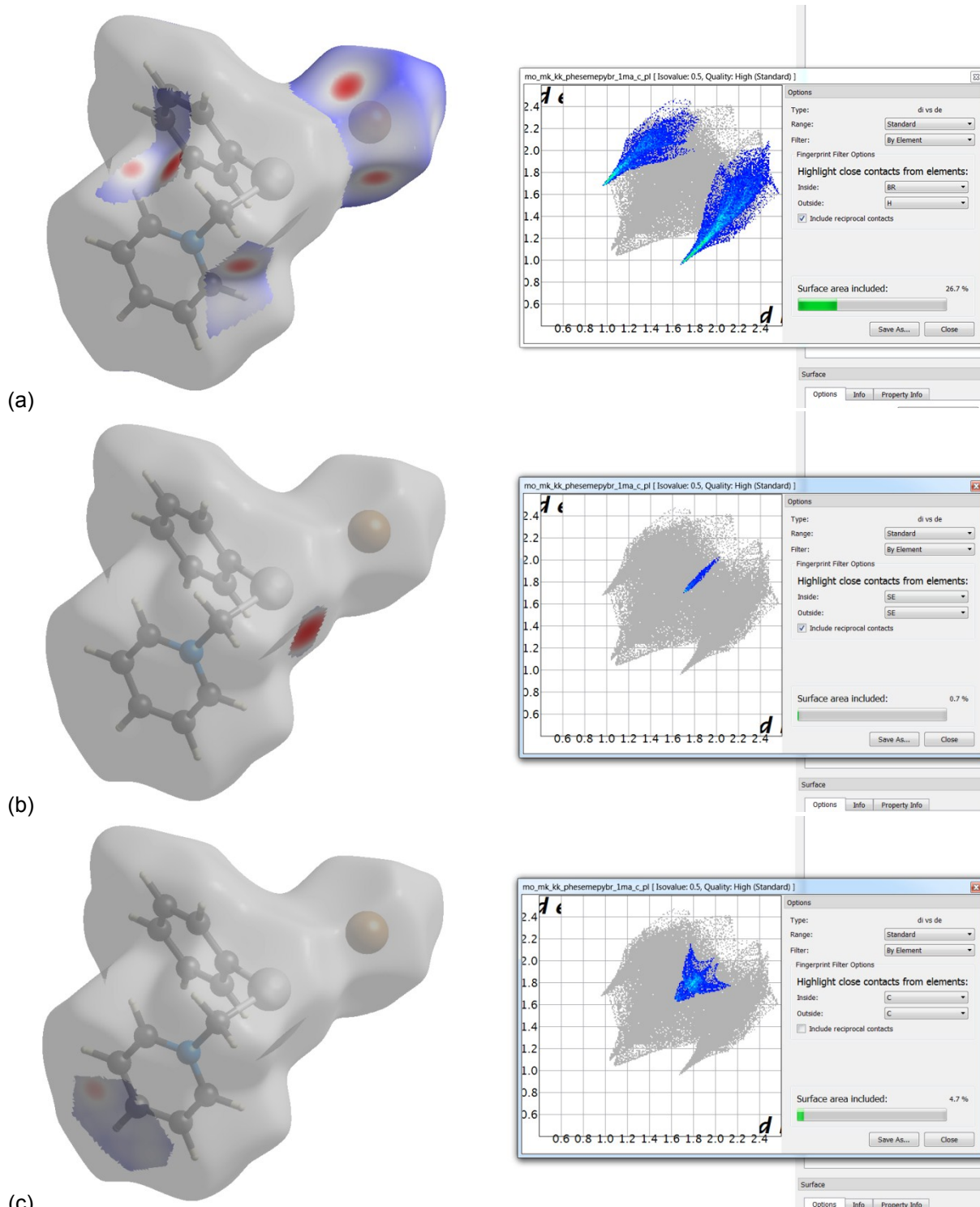
(c)

Figure S32. Relative contributions to the Hirshfeld surface area for the various close intermolecular contacts in **1-Br** as graphical presentation of Hirshfeld surface with 2D fingerprint plot (d_i – abscissa and d_e – ordinate are the distances from the surface to the nearest atom interior and exterior to the surface, respectively).

(a) Br$\cdots$H. A 2D fingerprint plot shows these C-H$\cdots$Br contacts, primarily from the CH_2 group as two sharp features pointing to the lower left of the plot, the upper one corresponding to the H-bond donor, and the lower one to the acceptor.[5b]

(b) Se$\cdots$Se.

(c) C$\cdots$C (i.e. $\pi\cdots\pi$). The pyridyl ring is involved in $\pi\cdots\pi$ interaction with a symmetry related one. The light-blue region near $d_e = d_i \approx 1.8$ Å on the diagonal indicates significant $\pi\cdots\pi$ interactions.[5b]
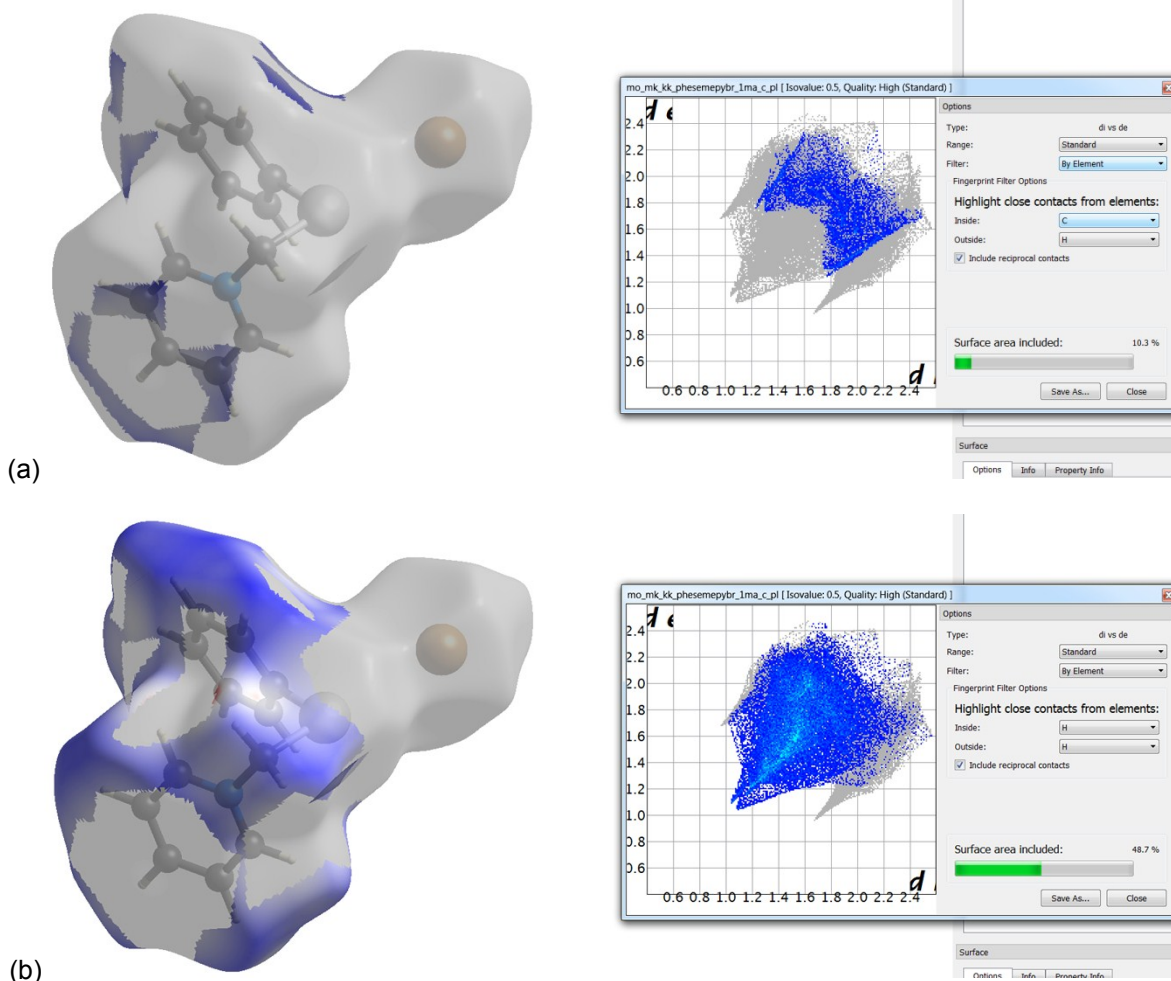
Figure S33. Relative contributions to the Hirshfeld surface area for the various close intermolecular contacts in **1-Br** as graphical presentation of Hirshfeld surface with 2D fingerprint plot (d_i – abscissa and d_e – ordinate are the distances from the surface to the nearest atom interior and exterior to the surface, respectively).

(a) C⋯H. No significant C–H⋯π interactions, as 'wings' at the upper left and lower right in the 2D fingerprint plot that are characteristic of stronger C–H⋯ π interactions are almost absent.[5b]

(b) H⋯H.

N-methyl-N'-[(Phenylseleno)methylene)]imidazolium tetraphenylborate (2-BPh₄)
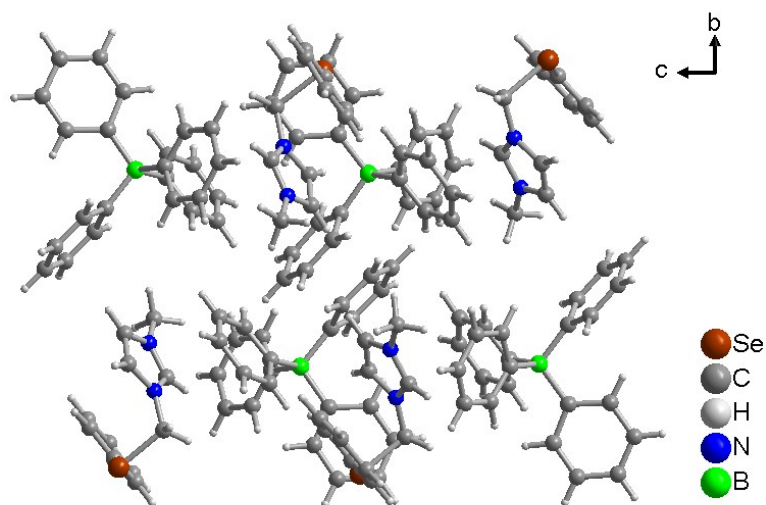
Figure S34. Full asymmetric unit of the compound **2-BPh₄**.
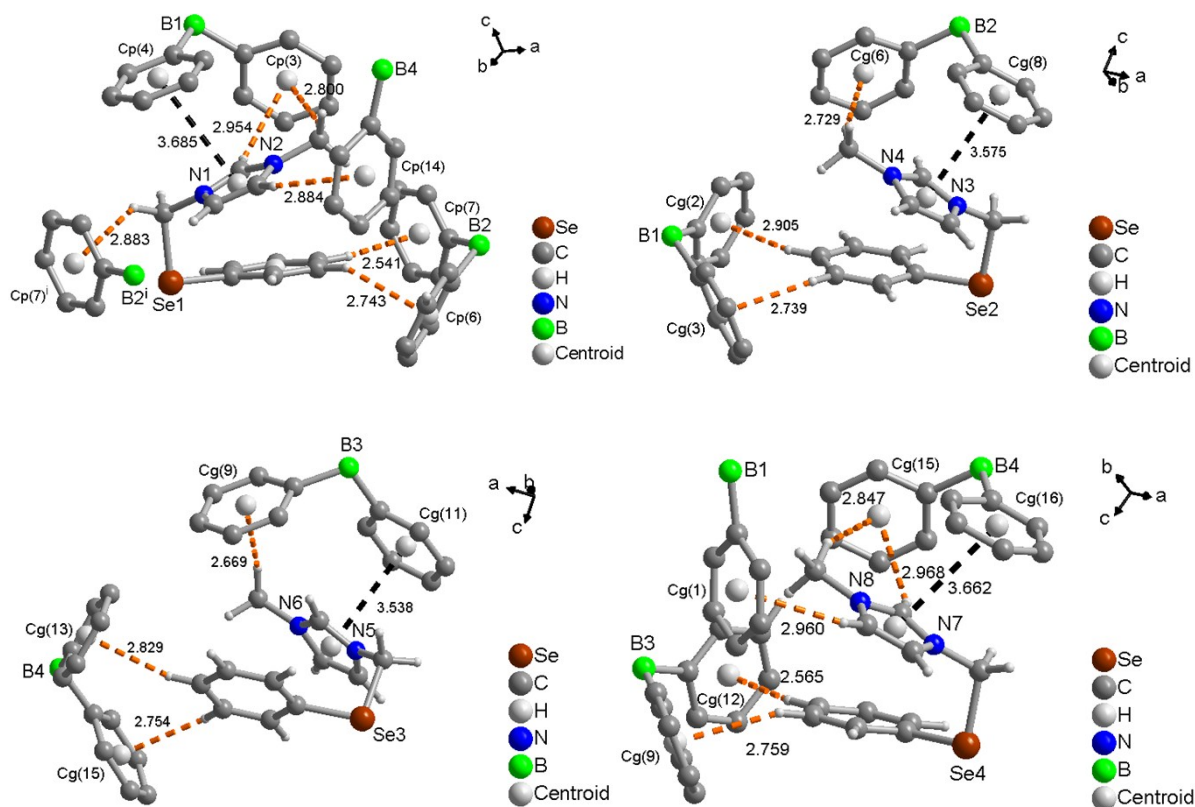
Figure S35. Short C-H⋯π distances (orange dashed lines) and short π–π-contacts (black dashed lines) of each cation of compound **2-BPh₄** (only the relevant parts of the anions shown, H-atoms of the anions have been omitted for clarity).

Table S6. Analysis of Short Ring-Interactions of compound **2-BPh₄** with Cg-Cg Distances < 6.0 Ang., Alpha < 20.000 Deg. and Beta < 60.0 Deg.

- Cg(I)   = Plane number I (= ring number in () above)
- Alpha   = Dihedral Angle between Planes I and J (Deg)
- Beta   = Angle Cg(I)-->Cg(J) or Cg(I)-->Me vector and normal to plane I (Deg)
- Gamma   = Angle Cg(I)-->Cg(J) vector and normal to plane J (Deg)
- Cg-Cg   = Distance between ring Centroids (Ang.)
- CgI_Perp = Perpendicular distance of Cg(I) on ring J (Ang.)
- CgJ_Perp = Perpendicular distance of Cg(J) on ring I (Ang.)
- Slippage = Distance between Cg(I) and Perpendicular Projection of Cg(J) on Ring I (Ang).

Cg(I)	Res(I)	Cg(J)	[ARU(J)]	Cg-Cg	Alpha	Beta	Gamma	CgI_Perp	CgJ_Perp	Slippage
Cg(4)	[1] ->	Cg(17)	[1556.05]	3.6852(2)	8	28.8	20.8	-3.4446	3.2280	1.778
Cg(8)	[2] ->	Cg(19)	[1555.06]	3.5755(2)	4	25.2	22.2	-3.3106	3.2347	1.523
Cg(11)	[3] ->	Cg(21)	[1555.07]	3.5383(2)	2	24.3	22.5	-3.2695	3.2256	1.454
Cg(12)	[3] ->	Cg(7)	[1655.02]	5.9779(4)	11	57.9	65.6	-2.4678	3.1793	5.062
Cg(16)	[4] ->	Cg(23)	[1556.08]	3.6616(2)	6	29.1	23.2	-3.3648	3.2002	1.779
Cg(17)	[5] ->	Cg(4)	[1554.01]	3.6851(2)	8	20.8	28.8	3.2280	-3.4446	1.310
Cg(19)	[6] ->	Cg(8)	[1555.02]	3.5755(2)	4	22.2	25.2	3.2347	-3.3106	1.351
Cg(21)	[7] ->	Cg(11)	[1555.03]	3.5383(2)	2	22.5	24.3	3.2256	-3.2695	1.353
Cg(23)	[8] ->	Cg(16)	[1554.04]	3.6616(2)	6	23.2	29.1	3.2002	-3.3648	1.444
			Min or Max	3.538	2.5	3.4	89.8	-5.142	-5.142	

[1555] = X,Y,Z
[1655] = 1+X,Y,Z
[1556] = X,Y,1+Z
[1455] = -1+X,Y,Z
[1554] = X,Y,-1+Z
(Significant contacts are highlighted in <mark>yellow</mark> – reciprocal contacts are not highlighted)

Cg(4) = C(30)–C(31)–C(32)–C(33)–C(34)–C(35)
Cg(8) = C(65)–C(66)–C(67)–C(68)–C(69)–C(70)
Cg(11) = C(94)–C(95)–C(96)–C(97)–C(98)–C(99)
Cg(16) = C(135)–C(136)–C(137)–C(138)–C(139)–C(140)
Cg(17) = N(1)–C(3)–C(2)–N(2)–C(4)
Cg(19) = N(3)–C(38)–C(37)–N(4)–C(39)
Cg(21) = N(5)–C(72)–C(73)–N(6)–C(74)
Cg(23) = N(7)–C(108)–C(107)–N(8)–C(109)

Table S7. Analysis of X-H...Cg(Pi-Ring) Interactions of compound **2-BPh$_4$** (H..Cg < 3.0 Ang. - Gamma < 30.0 Deg)

- Cg(J)   = Center of gravity of ring J (Plane number above)
- H-Perp = Perpendicular distance of H to ring plane J
- Gamma   = Angle between Cg-H vector and ring J normal
- X-H..Cg = X-H-Cg angle (degrees)
- X..Cg   = Distance of X to Cg (Angstrom)
- X-H, Pi = Angle of the X-H bond with the Pi-plane (i.e.' Perpendicular = 90 degrees, Parallel = 0 degrees)

X-H(I)	Res(I)	Cg(J)	[ARU(J)]	H..Cg	H-Perp	Gamma	X-H..Cg	X..Cg	X-H,Pi
C(1)-H(1C)	[5]	-> Cg(3)	[1554.01]	2.80	2.50	26.89	157	3.7234(2)	79
C(2)-H(2)	[5]	-> Cg(14)	[2646.04]	2.89	2.68	21.69	146	3.7085(2)	66
C(4)-H(4)	[5]	-> Cg(3)	[1554.01]	2.95	2.64	26.64	140	3.7301(2)	75
C(5)-H(5B)	[5]	-> Cg(7)	[1655.02]	2.88	-2.68	21.50	136	3.6630(2)	67
C(7)-H(7)	[5]	-> Cg(17)	[1555.05]	2.99	2.97	7.82	102	3.3247(2)	9
C(8)-H(8)	[5]	-> Cg(6)	[1555.02]	2.74	-2.70	10.19	148	3.5873(2)	53
C(9)-H(9)	[5]	-> Cg(7)	[1555.02]	2.54	2.54	2.88	170	3.4806(2)	82
C(106)-H(10A)	[8]	-> Cg(15)	[1554.04]	2.85	2.54	26.69	150	3.7269(2)	71
C(36)-H(36B)	[6]	-> Cg(6)	[1555.02]	2.73	2.59	18.70	165	3.6844(2)	82
C(44)-H(44)	[6]	-> Cg(2)	[1555.01]	2.90	-2.72	20.70	144	3.7138(2)	71
C(45)-H(45)	[6]	-> Cg(3)	[1555.01]	2.74	-2.72	6.14	142	3.5366(2)	52
C(71)-H(71A)	[7]	-> Cg(9)	[1555.03]	2.67	2.56	16.18	159	3.5992(2)	74
C(78)-H(78)	[7]	-> Cg(15)	[1655.04]	2.75	-2.74	6.25	145	3.5747(2)	52
C(79)-H(79)	[7]	-> Cg(13)	[1655.04]	2.83	-2.71	16.73	150	3.6827(2)	71
C(107)-H(107)	[8]	-> Cg(1)	[2656.01]	2.96	2.73	22.94	146	3.7851(2)	67
C(109)-H(109)	[8]	-> Cg(15)	[1554.04]	2.97	2.67	26.04	141	3.7548(2)	75
C(114)-H(114)	[8]	-> Cg(12)	[1455.03]	2.57	2.56	5.03	163	3.4852(2)	77
C(115) -H(115)	[8]	-> Cg(9)	[1455.03]	2.76	-2.73	8.58	153	3.6284(2)	54
C(120)-H(120)	[4]	-> Cg(18)	[1555.05]	2.95	2.85	14.78	148	3.7881(2)	68
		Min or Max		2.540	-2.738	2.9	170.00	3.325	82.00

[1554] = X,Y,-1+Z
[2646] = 1-X,-1/2+Y,1-Z
[1655] = 1+X,Y,Z
[1555] = X,Y,Z
[2656] = 1-X,1/2+Y,1-Z
[1455] = -1+X,Y,Z
(significant contacts are highlighted in <mark>yellow</mark>, potential contacts are highlighted in <mark>green</mark>)

Cg(3) = C(24)–C(25)–C(26)–C(27)–C(28)–C(29)
Cg(6) = C(53)–C(54)–C(55)–C(56)–C(57)–C(58)
Cg(7) = C(59)–C(60)–C(61)–C(62)–C(63)–C(64)
Cg(9) = C(82)–C(83)–C(84)–C(85)–C(86)–C(87)
Cg(12) = C(100)–C(101)–C(102)–C(103)–C(104)–C(105)
Cg(14) = C(123)–C(124)–C(125)–C(126)–C(127)–C(128)
Cg(15) = C(129)–C(130)–C(131)–C(132)–C(133)–C(134)

In the solid-state structure of $(PhSeCH_2)MeIm^+ BPh_4^-$, **2-BPh₄** there are four independent ion pairs in the asymmetric unit. For simplicity these four ion pairs have been analyzed with their enveloping Hirshfeld surface (Figure S36). This enveloping will not give the supramolecular interactions among the four independent ion pairs but we can assume that the interactions from the four independent ion pairs to the surrounding symmetry related ion pairs also reflect the interactions among the independent ones.

The Hirshfeld surface (d_{norm}) **2-BPh₄** displays close intermolecular contacts around CH and CH_2 hydrogen atoms (red spots on the d_{norm} surface) (Figure S36(a)). The majority of the surface is colored blue (representing the sum of longer than van-der-Waals contact distances). The relative contributions to the Hirshfeld surface area due to close intermolecular contacts are summarized in Table S5.
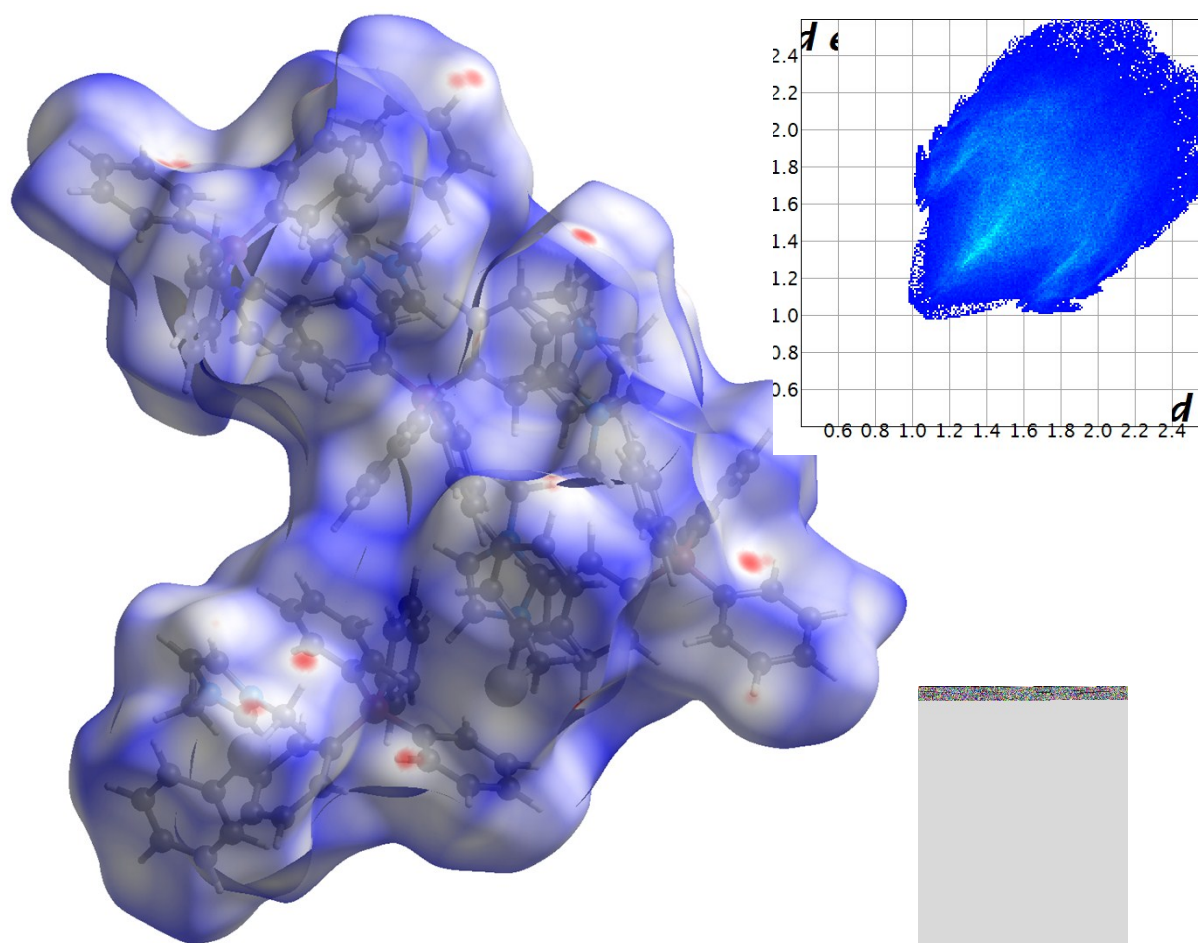
Figure S36. (a) Hirshfeld surface of **2-BPh₄** mapped with the d_{norm} property.[5c] Red represents the closest contacts, and blue the most distant contacts.
(b) 2D fingerprint plot of **2-BPh₄**. d_i (abscissa) and d_e (ordinate) are the distances from the surface to the nearest atom interior and exterior to the surface, respectively. For a breakdown of the fingerprint plot into the contributions from Se···all, C···H, H···H close intermolecular contacts (see Table S8 and Figure S37 and S38).

Table S8. Percent contributions of close supramolecular interactions to Hirshfeld surface in **2-BPh$_4$**.[a]

Interaction (inside⋯outside)	**Percent (%)**	**Figure**
Se⋯all and all⋯Se	7.1	Figure 37
C⋯H (i.e. C–H⋯π) [a]	25.1	Figure 38(a)
H⋯H [a]	67.8	Figure 38(b)
Sum	100	

[a] includes reciprocal contacts.
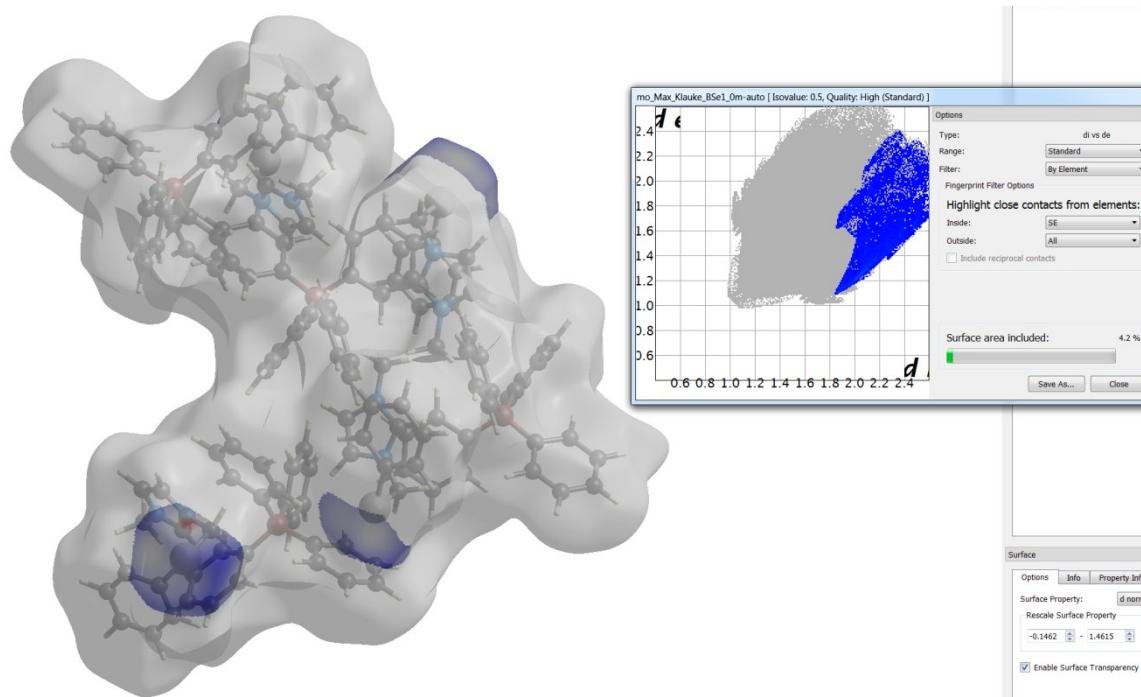
Figure S37. Relative contributions to the Hirshfeld surface area for the various close intermolecular contacts in **2-BPh$_4$** as graphical presentation of Hirshfeld surface with 2D fingerprint plot (d_i – abscissa and d_e – ordinate are the distances from the surface to the nearest atom interior and exterior to the surface, respectively).

The share of Se⋯all is 4.7%, the one of all⋯Se is 2.9%, together 7.1%.

(a)

(b)
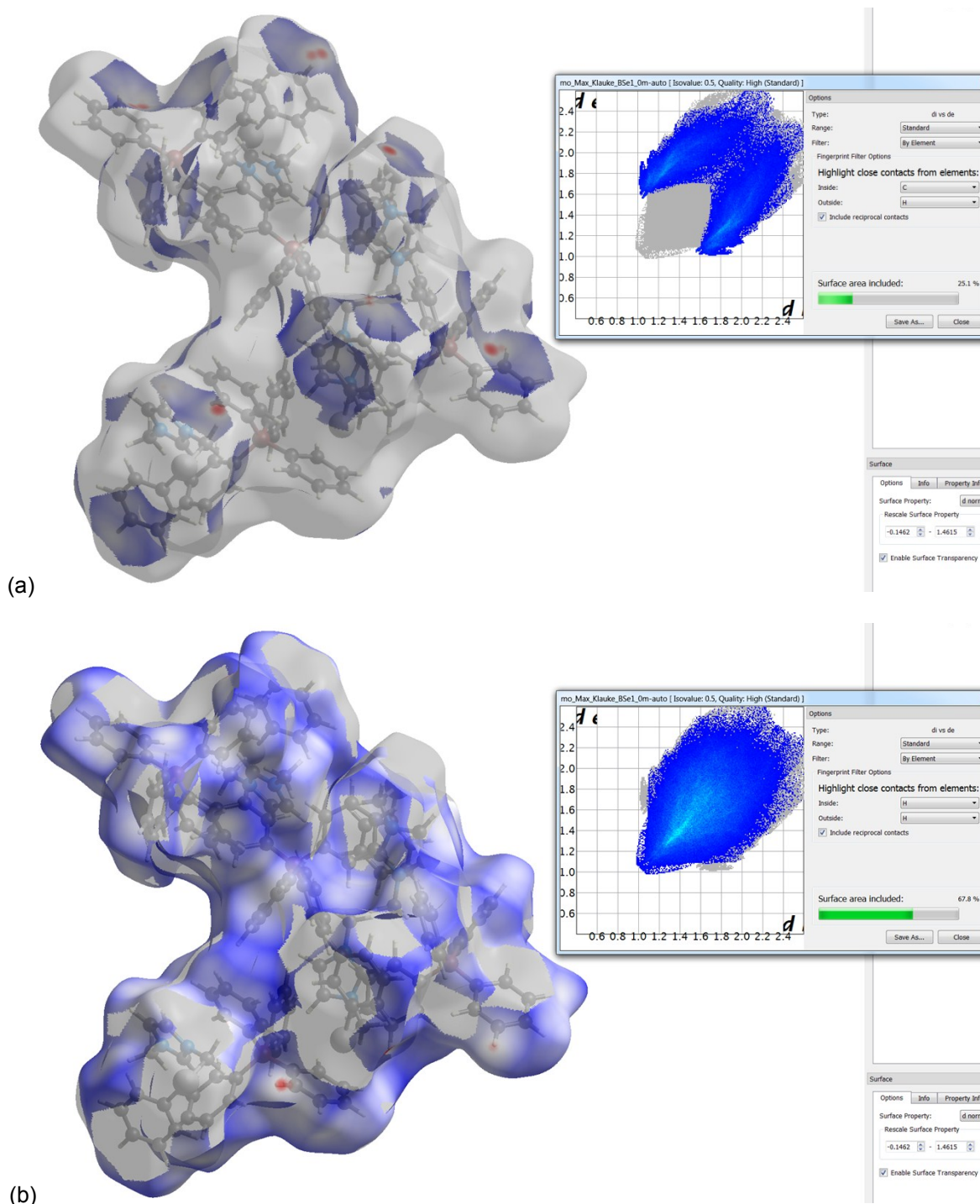
Figure S38. Relative contributions to the Hirshfeld surface area for the various close intermolecular contacts in **2-BPh₄** as graphical presentation of Hirshfeld surface with 2D fingerprint plot (d_i – abscissa and d_e – ordinate are the distances from the surface to the nearest atom interior and exterior to the surface, respectively).

(a) C···H. Significant C–H···π interactions, as 'Wings' at the upper left and lower right in the 2D fingerprint plot that are characteristic of stronger C–H···π interactions.[5b]

(b) H···H.

_N_-butyl-_N'_-[(Phenylseleno)methylene)]imidazolium tetraphenylborate (3-BPh$_4$)
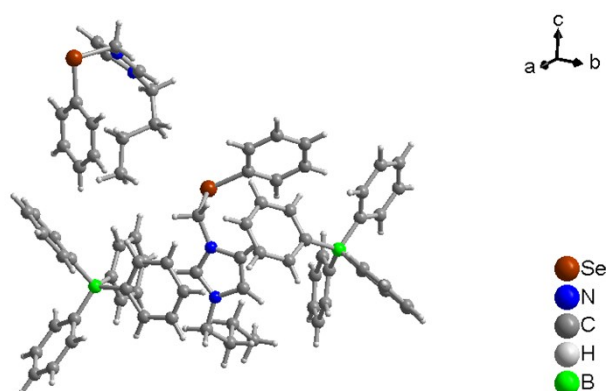
Figure S39. Full asymmetric unit of compound **3-BPh$_4$**.
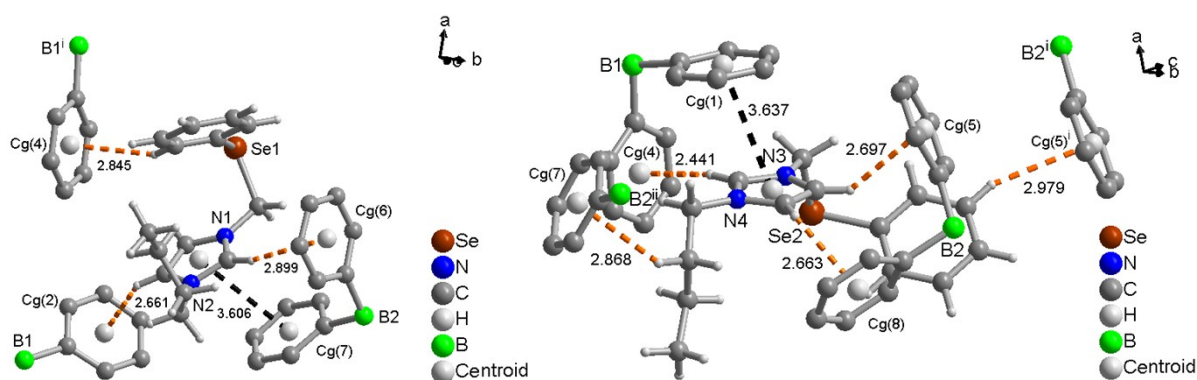
Figure S40. Short C-H···π contact (orange dashed lines) and short π–π-contacts (black dashed lines) of each cation of compound **3-BPh$_4$** (only the relevant parts of the anions shown, H-Atoms of the anions have been omitted for clarity).

Table S9. Analysis of Short Ring-Interactions with Cg-Cg Distances < 6.0 Ang., Alpha < 20.000 Deg. and Beta < 60.0 Deg.

- Cg(I)   = Plane number I (= ring number in () above)
- Alpha   = Dihedral Angle between Planes I and J (Deg)
- Beta   = Angle Cg(I)-->Cg(J) or Cg(I)-->Me vector and normal to plane I (Deg)
- Gamma   = Angle Cg(I)-->Cg(J) vector and normal to plane J (Deg)
- Cg-Cg   = Distance between ring Centroids (Ang.)
- CgI_Perp = Perpendicular distance of Cg(I) on ring J (Ang.)
- CgJ_Perp = Perpendicular distance of Cg(J) on ring I (Ang.)
- Slippage = Distance between Cg(I) and Perpendicular Projection of Cg(J) on Ring I (Ang.).

Cg(I)	Res(I)	Cg(J)	[ARU(J)]	Cg-Cg	Alpha	Beta	Gamma	CgI_Perp	CgJ_Perp	Slippage
Cg(1)	[1] -> Cg(11)	[1555.04]	3.6369(18)	8.45(16)	18.7	27.1	3.2369(14)	-3.4441(12)	1.778
Cg(7)	[2] -> Cg(9)	[3666.03]	3.6059(19)	6.70(17)	22.5	28.8	3.1597(13)	3.3318(13)	1.523
Cg(8)	[2] -> Cg(8)	[3565.02]	5.526(3)	0.0(2)	56.2	56.2	3.0717(18)	3.0716(18)	4.594
Cg(9)	[3] -> Cg(7)	[3666.02]	3.6056(19)	6.70(17)	28.8	22.5	3.3316(13)	3.1597(13)	1.737
Cg(11)	[4] -> Cg(1)	[1555.01]	3.6368(18)	8.45(16)	27.1	18.7	-3.4441(12)	3.2369(14)	1.658
			Min or Max	3.538	0.0	2.5	89.4	-4.811	-5.900	

[1555] = X,Y,Z
[3666] = 1-X,1-Y,1-Z
[3565] = -X,1-Y,-Z

(Significant contacts are highlighted in <mark>yellow</mark> – reciprocal contacts are not highlighted)

Cg(1) = C(15)–C(16)–C(17)–C(18)–C(19)–C(20)
Cg(7) = C(65)–C(66)–C(67)–C(68)–C(69)–C(70)
Cg(9) = N(1)–C(6)–C(5)–N(2)–C(7)
Cg(11) = N(3)–C(44)–C(43)–N(4)–C(45)

Table S10. Analysis of X-H...Cg(Pi-Ring) Interactions (H..Cg < 3.0 Ang. - Gamma < 30.0 Deg)

- Cg(J)   = Center of gravity of ring J (Plane number above)
- H-Perp = Perpendicular distance of H to ring plane J
- Gamma   = Angle between Cg-H vector and ring J normal
- X-H..Cg = X-H-Cg angle (degrees)
- X..Cg   = Distance of X to Cg (Angstrom)
- X-H, Pi = Angle of the X-H bond with the Pi-plane (i.e.' Perpendicular = 90 degrees, Parallel = 0 degrees)

X-H(I)	Res(I) Cg(J)	[ARU(J)]	H..Cg	H-Perp	Gamma	X-H..Cg	X..Cg	X-H,Pi
C(5)-H(5)	[3] -> Cg(2)	[4455.01]	2.66	-2.65	5.11	133	3.385(4)	42
C(7)-H(7)	[3] -> Cg(6)	[3666.02]	2.90	2.80	14.92	165	3.823(4)	88
C(14)-H(14A)	[3] -> Cg(4)	[4555.01]	2.84	-2.84	4.00	147	3.678(4)	61
C(41)-H(41A)	[4] -> Cg(7)	[3665.02]	2.87	-2.79	13.38	139	3.676(4)	62
C(43)-H(43)	[4] -> Cg(8)	[1555.02]	2.66	2.55	16.64	125	3.305(4)	51
C(44)-H(44)	[4] -> Cg(6)	[1555.02]	2.70	-2.58	17.23	138	3.462(3)	65
C(45)-H(45)	[4] -> Cg(4)	[1555.01]	2.44	2.42	6.91	169	3.378(3)	83
C(51)-H(51)	[4] -> Cg(5)	[3666.02]	2.98	2.81	19.58	159	3.884(4)	58
	Min or Max		2.440	-2.838	4.0	169.00	3.305	88.00

[4455] = -1/2+X,1/2-Y,1/2+Z
[3666] = 1-X,1-Y,1-Z
[4555] = 1/2+X,1/2-Y,1/2+Z
[3665] = 1-X,1-Y,-Z
[1555] = X,Y,Z

(significant contacts are highlighted in <mark>yellow</mark>, potential contacts are highlighted in <mark>green</mark>)

Cg(2) = C(21)–C(22)–C(23)–C(24)–C(25)–C(26)
Cg(4) = C(33)–C(34)–C(35)–C(36)–C(37)–C(38)
Cg(6) = C(59)–C(60)–C(61)–C(62)–C(63)–C(64)
Cg(8) = C(71)–C(72)–C(73)–C(74)–C(75)–C(76)

In the solid-state structure of (PhSeCH$_2$)BuIm$^+$ BPh$_4^-$, **3-BPh$_4$** there are two independent ion pairs in the asymmetric unit. For simplicity these four ion pairs have been analyzed with their enveloping Hirshfeld surface (Figure S41). This enveloping will not give the supramolecular interactions among the two independent ion pairs but we can assume that the interactions from the two independent ion pairs to the surrounding symmetry related ion pairs also reflect the interactions among the independent ones.

The Hirshfeld surface (d$_{norm}$) **3-BPh$_4$** displays close intermolecular contacts around CH and CH$_2$ hydrogen atoms (red spots on the d$_{norm}$ surface) (Figure S41(a)). The most part of the surface is colored blue (representing the sum of longer than van-der-Waals contact distances). The relative contributions to the Hirshfeld surface area due to close intermolecular contacts are summarized in Table S11.
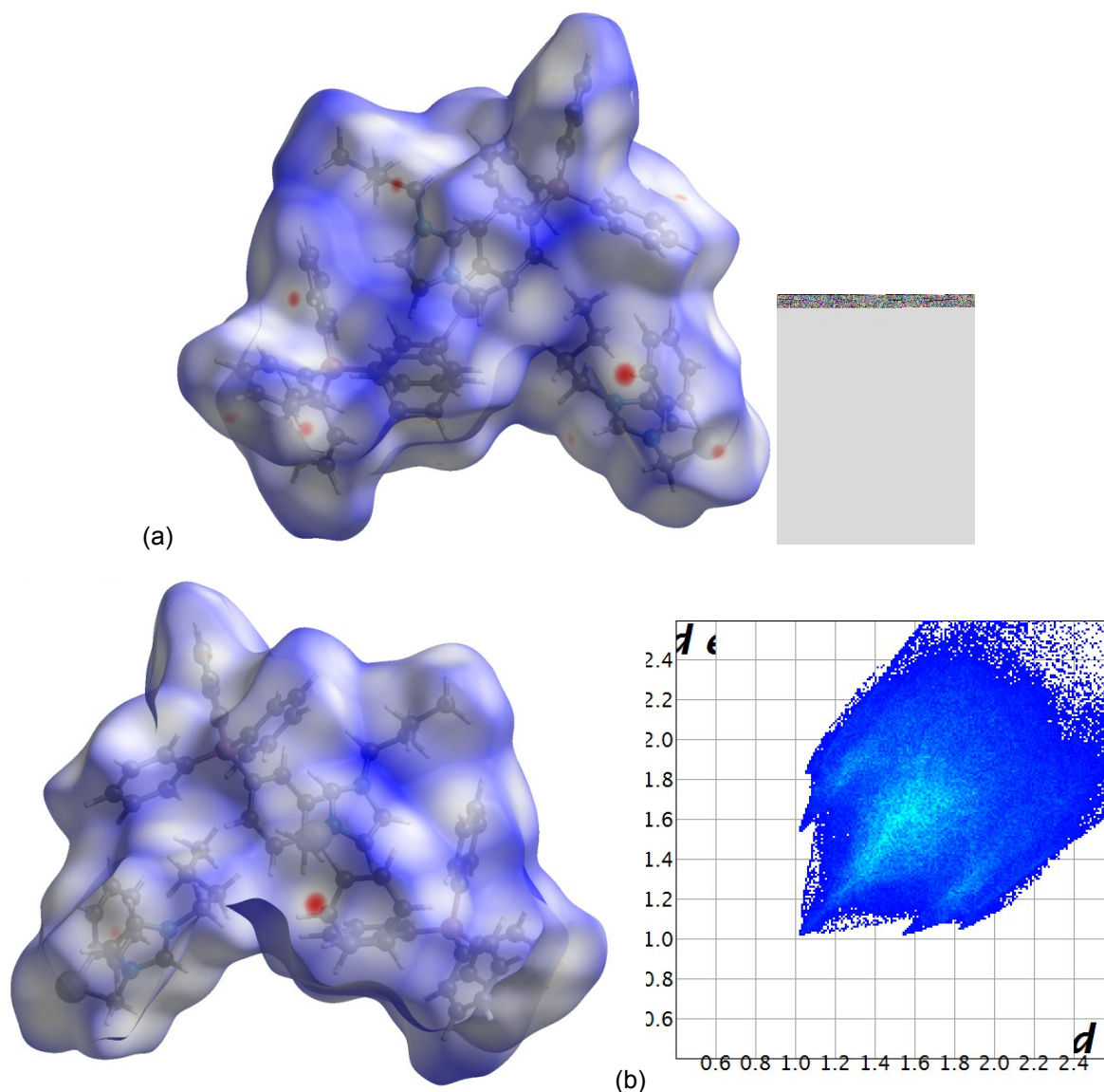
Figure S41. (a) Hirshfeld surface of **3-BPh₄** mapped with the d_{norm} property – with two views from opposite side.[5c] Red represents the closest contacts, and blue the most distant contacts.

(b) 2D fingerprint plot of **3-BPh₄**. d_i (abscissa) and d_e (ordinate) are the distances from the surface to the nearest atom interior and exterior to the surface, respectively. For a breakdown of the fingerprint plot into the contributions from Se···all, C···H, H···H close intermolecular contacts (see Table S11 and Figure S42 and S43).

Table S11. Percent contributions of close supramolecular interactions to Hirshfeld surface in **3-BPh₄**.ᵃ

Interaction (inside···outside)	Percent (%)	Figure
Se···all and all···Se	5.5	Figure S41
C···H (i.e. C–H···p) [a]	23.1	Figure S43(a)
H···H [a]	70.2	Figure S43(b)
Sum	98.8	

[a] includes reciprocal contacts.
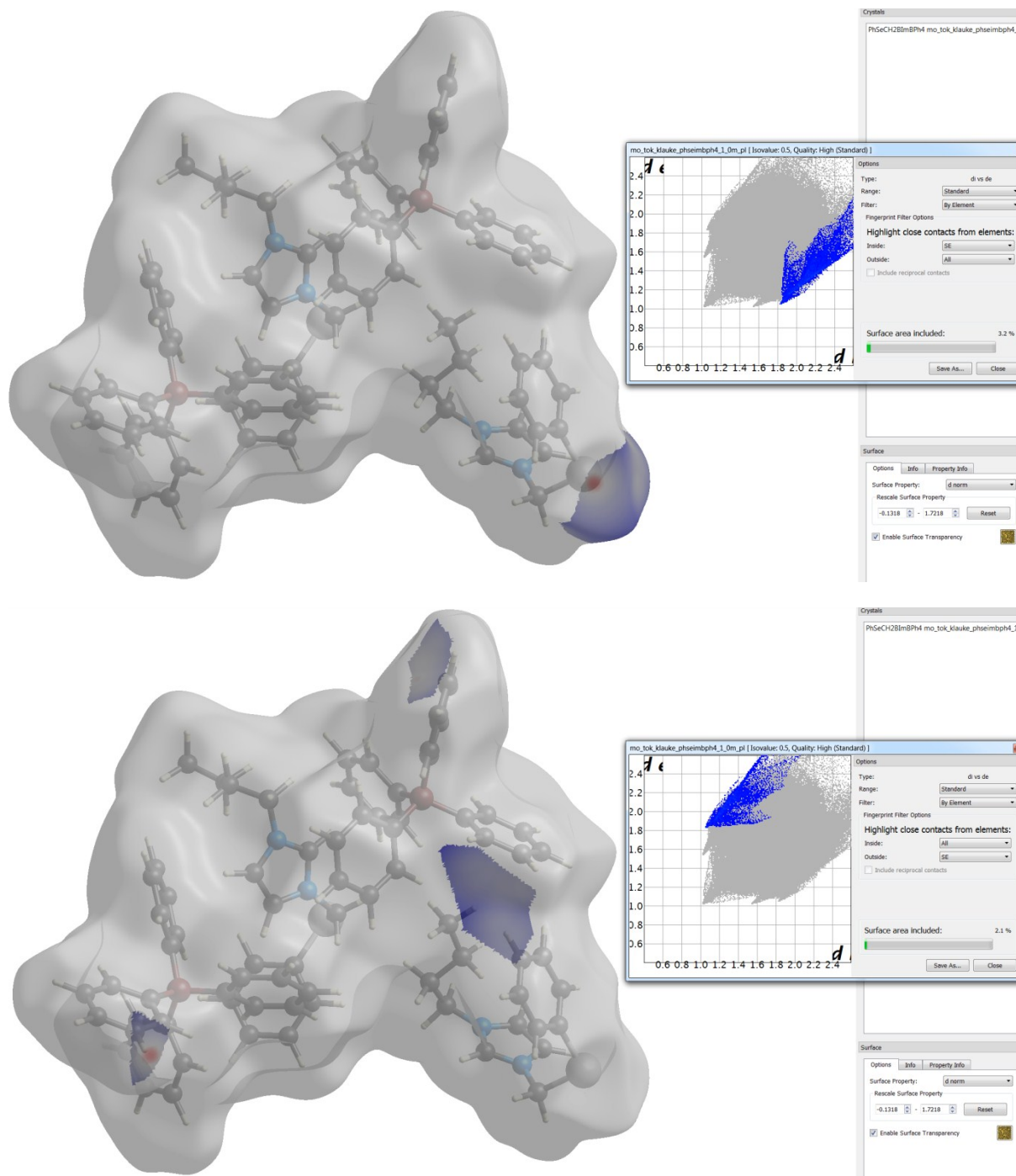
Figure S42. Relative contributions to the Hirshfeld surface area for the various close intermolecular contacts in **3-BPh₄** as graphical presentation of Hirshfeld surface with 2D fingerprint plot (d_i – abscissa and d_e – ordinate are the distances from the surface to the nearest atom interior and exterior to the surface, respectively).

The share of Se···all is 3.2%, the one of all···Se is 2.1%, together 5.3%.

(a)

(b)
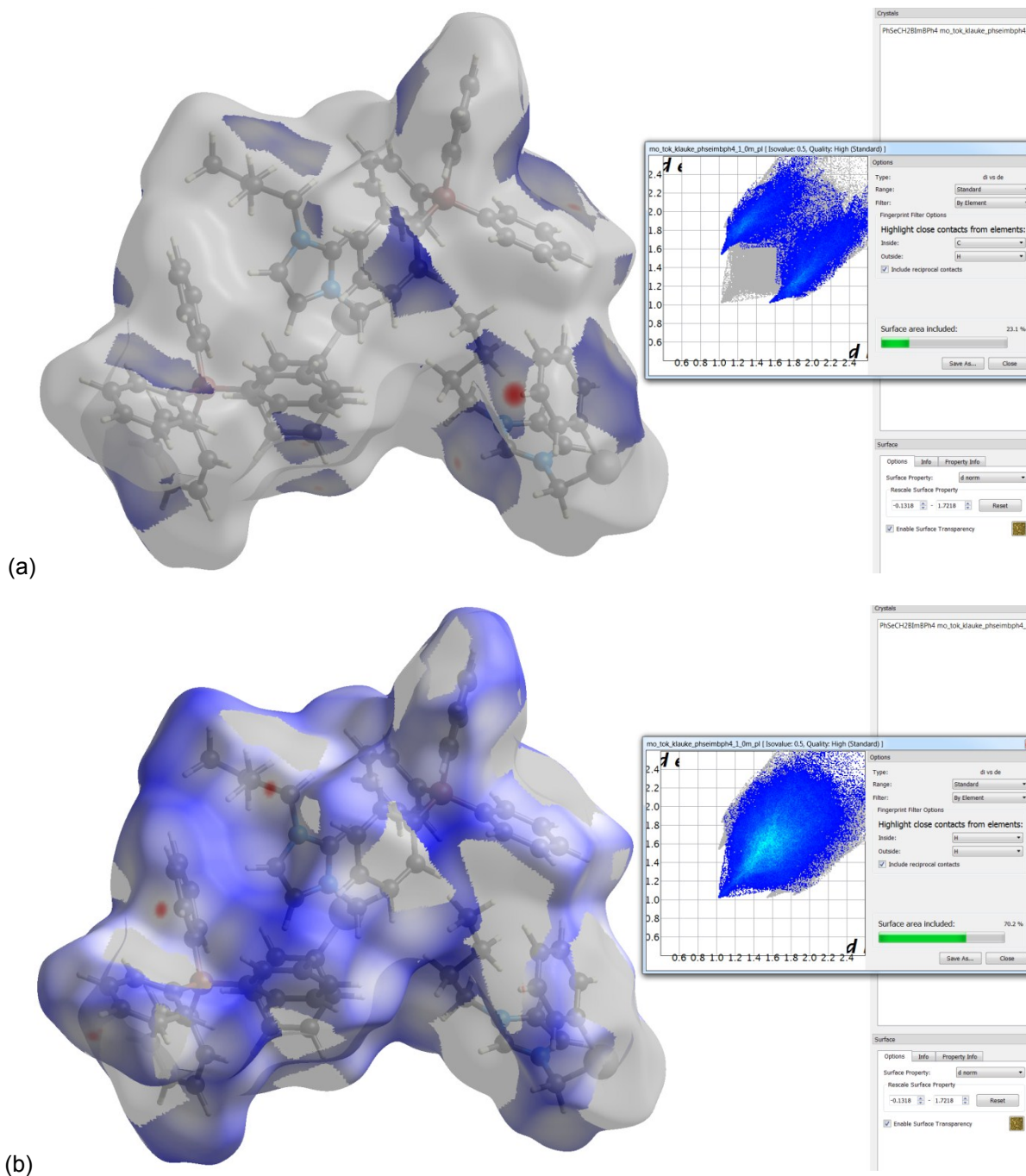
Figure S43. Relative contributions to the Hirshfeld surface area for the various close intermolecular contacts in **3-BPh₄** as graphical presentation of Hirshfeld surface with 2D fingerprint plot (d_i – abscissa and d_e – ordinate are the distances from the surface to the nearest atom interior and exterior to the surface, respectively).

(a) C···H. 'Wings' at the upper left and lower right in the 2D fingerprint plot that are characteristic of stronger C–H···p interactions are not very prominent.[5b]

(b) H···H.

Results of the density measurements

Table S12. Density measurements for the three ILs **1-**, **2-** and **3-NTf$_2$**.

T / K	p / bar	ρ / kg/m^3
1-NTf$_2$		
298.15	1	1601.64
313.15	1	1584.49
323.15	1	1573.27
333.15	1	1563.66
2-NTf$_2$ [a]		
298.15	1	849.25
313.15	1	832.60
323.15	1	822.00
333.14	1	810.25
3-NTf$_2$		
298.15	1	1511.94
313.15	1	1497.35
323.15	1	1489.02
333.15	1	1478.64

[a] mixed density with ACN, 14.78 w% 3-NTf$_2$

II   Results of the QCM-measurements

Table S13. Results for vapor pressure temperature dependence and vaporization enthalpies $\Delta_l^g H_m^o(T)$ determined by QCM for studied ionic liquids.

Run	T / K	$10^6 \cdot p^*_{sat}$ / Pa	T^{-1} / K^{-1}	$R \cdot \ln(p^*_{sat}/p^o)$	$\dfrac{\Delta_l^g H_m^o(T)}{\text{kJ} \cdot \text{mol}^{-1}}$
			2-NTf$_2$		
	$\ln\left(p^*_{sat}/p^o\right) = -\dfrac{73804}{R} - \dfrac{123618}{R}\left(\dfrac{1}{T} - \dfrac{1}{T_0}\right) - \dfrac{95}{R}\left(\dfrac{T_0}{T} - 1 - \ln\left(\dfrac{T}{T_0}\right)\right)$, $T_0 = 388.1$ K				
	402.89	47	0.002482	-178.6	122.2
	398.20	30	0.002511	-182.3	122.7
	393.42	20	0.002542	-185.8	123.1
1	388.57	13	0.002574	-189.5	123.6
	383.67	7.8	0.002606	-193.5	124.0
	378.70	4.5	0.002641	-198.1	124.5
	373.74	2.7	0.002676	-202.4	125.0
	368.76	1.5	0.002712	-207.1	125.4
	402.98	47	0.002481	-178.6	122.2
	398.28	31	0.002511	-182.1	122.7
	393.49	20	0.002541	-185.7	123.1
2	388.63	12	0.002573	-189.9	123.6
	383.70	7.5	0.002606	-193.9	124.0
	378.74	4.5	0.002640	-198.1	124.5
	373.83	2.7	0.002675	-202.4	125.0
	405.46	60	0.002466	-176.6	122.0
	400.75	39	0.002495	-180.1	122.4
	395.88	24	0.002526	-184.0	122.9
3	391.05	16	0.002557	-187.7	123.3
	386.19	9.8	0.002589	-191.6	123.8
	381.28	5.9	0.002623	-195.9	124.3
	376.33	3.4	0.002657	-200.4	124.7
			3-NTf$_2$		
	$\ln\left(p^*_{sat}/p^o\right) = -\dfrac{76617}{R} - \dfrac{132004}{R}\left(\dfrac{1}{T} - \dfrac{1}{T_0}\right) - \dfrac{121}{R}\left(\dfrac{T_0}{T} - 1 - \ln\left(\dfrac{T}{T_0}\right)\right)$, $T_0 = 391.3$ K				
	413.14	50	0.002420	-178.0	129.4
	408.26	32	0.002449	-181.9	130.0
	403.39	20	0.002479	-185.7	130.5
	398.48	12	0.002510	-189.8	131.1
1	393.57	7.5	0.002541	-193.8	131.7
	388.62	4.4	0.002573	-198.2	132.3
	383.65	2.6	0.002607	-202.7	132.9
	378.67	1.5	0.002641	-207.3	133.5
	373.68	0.87	0.002676	-211.8	134.1
	368.69	0.47	0.002712	-216.8	134.7
	415.59	61	0.002406	-176.4	129.1
	410.77	39	0.002434	-180.0	129.7
	405.91	25	0.002464	-183.9	130.2
2	400.92	15	0.002494	-187.9	130.8
	396.00	9.4	0.002525	-192.0	131.4
	391.06	5.8	0.002557	-196.0	132.0
	386.08	3.4	0.002590	-200.4	132.6

	381.08	2.0	0.002624	-204.8	133.2
	376.07	1.1	0.002659	-209.5	133.9
	371.08	0.66	0.002695	-214.0	134.5
3	413.03	50	0.002421	-178.1	129.4
	408.25	32	0.002449	-181.8	130.0
	403.49	20	0.002478	-185.6	130.5
	398.56	12	0.002509	-189.7	131.1
	393.68	7.5	0.002540	-193.8	131.7
	388.78	4.4	0.002572	-198.3	132.3
	383.83	2.7	0.002605	-202.4	132.9
	378.84	1.5	0.002640	-207.0	133.5
	373.80	0.88	0.002675	-211.7	134.1
	368.76	0.46	0.002712	-217.0	134.7

1-NTf$_2$

$$\ln\left(p_{\mathrm{sat}}^{*}/p^{\mathrm{o}}\right)=-\frac{80356}{R}-\frac{155202}{R}\left(\frac{1}{T}-\frac{1}{T_0}\right)-\frac{89}{R}\left(\frac{T_0}{T}-1-\ln\left(\frac{T}{T_0}\right)\right),\ T_0 = 407.3\ \mathrm{K}$$

1	423.03	29	0.002364	-182.6	153.8
	418.01	14	0.002392	-188.4	154.3
	412.99	6.9	0.002421	-194.5	154.7
	407.97	3.7	0.002451	-199.6	155.1
	402.96	2.4	0.002482	-203.4	155.6
	397.95	1.4	0.002513	-207.6	156.0
	392.82	0.86	0.002546	-211.9	156.5
	387.81	0.56	0.002579	-215.4	156.9
	382.80	0.35	0.002612	-219.2	157.4
	377.81	0.26	0.002647	-221.9	157.8
2	428.33	57	0.002335	-177.0	153.3
	423.32	27	0.002362	-183.1	153.8
	418.32	13	0.002390	-189.1	154.2
	413.33	6.5	0.002419	-195.0	154.7
	408.36	3.9	0.002449	-199.2	155.1
	403.38	2.4	0.002479	-203.4	155.6
	398.40	1.4	0.002510	-207.9	156.0
	393.41	1.0	0.002542	-210.7	156.4
3	433.40	194	0.002307	-166.8	152.9
	428.41	99	0.002334	-172.4	153.3
	423.42	43	0.002362	-179.3	153.8
	418.45	19	0.002390	-186.3	154.2
	413.44	4.7	0.002419	-197.7	154.7
	408.46	3.4	0.002448	-200.4	155.1
	403.47	2.0	0.002478	-204.9	155.5
	398.50	1.7	0.002509	-206.3	156.0
	393.51	1.2	0.002541	-209.4	156.4
4	433.10	110	0.002309	-171.5	152.9
	428.09	54	0.002336	-177.5	153.4
	423.07	19	0.002364	-185.9	153.8
	418.07	9.1	0.002392	-192.3	154.2
	412.95	5.9	0.002422	-195.9	154.7
	407.93	3.8	0.002451	-199.6	155.2
	402.92	3.1	0.002482	-201.2	155.6
	398.10	1.8	0.002512	-205.6	156.0
	393.32	1.2	0.002542	-209.2	156.5
	388.35	0.85	0.002575	-211.9	156.9

	[Ph-C$_4$mim][NTf$_2$] Ref [6]				

$$\ln\left(p_{\text{sat}}^*/p^{\text{o}}\right) = -\frac{73667}{R} - \frac{132275}{R}\left(\frac{1}{T} - \frac{1}{T_0}\right) - \frac{65}{R}\left(\frac{T_0}{T} - 1 - \ln\left(\frac{T}{T_0}\right)\right), \quad T_0 = 384.8 \text{ K}$$

1	407.99	102	0.002451	-172.1	130.8
	403.02	65	0.002481	-175.9	131.1
	397.90	39	0.002513	-180.0	131.4
	392.88	24	0.002545	-184.0	131.7
	387.84	14	0.002578	-188.6	132.1
	382.82	7.9	0.002612	-193.4	132.4
	377.80	4.6	0.002647	-198.0	132.7
	372.79	2.6	0.002682	-202.7	133.1
	367.79	1.5	0.002719	-207.3	133.4
	362.83	0.80	0.002756	-212.4	133.7
2	402.95	64	0.002482	-176.1	131.1
	397.90	38	0.002513	-180.3	131.4
	392.89	24	0.002545	-184.1	131.7
	387.82	13	0.002578	-189.0	132.1
	382.81	8.2	0.002612	-193.1	132.4
	377.78	4.5	0.002647	-198.1	132.7
	372.77	2.6	0.002683	-202.8	133.1
	367.76	1.5	0.002719	-207.2	133.4
	362.80	0.8	0.002756	-212.2	133.7
3	405.42	80	0.002467	-174.2	130.9
	400.37	50	0.002498	-178.1	131.3
	395.33	30	0.002530	-182.3	131.6
	390.31	18	0.002562	-186.5	131.9
	385.29	11	0.002595	-191.0	132.2
	380.26	6.1	0.002630	-195.5	132.6
	375.23	3.5	0.002665	-200.1	132.9
	370.22	1.9	0.002701	-205.2	133.2

	[C$_3$Py][NTf$_2$] Ref [7]				

$$\ln\left(p_{\text{sat}}^*/p^{\text{o}}\right) = -\frac{73469}{R} - \frac{128081}{R}\left(\frac{1}{T} - \frac{1}{T_0}\right) - \frac{66}{R}\left(\frac{T_0}{T} - 1 - \ln\left(\frac{T}{T_0}\right)\right), \quad T_0 = 398.2 \text{ K}$$

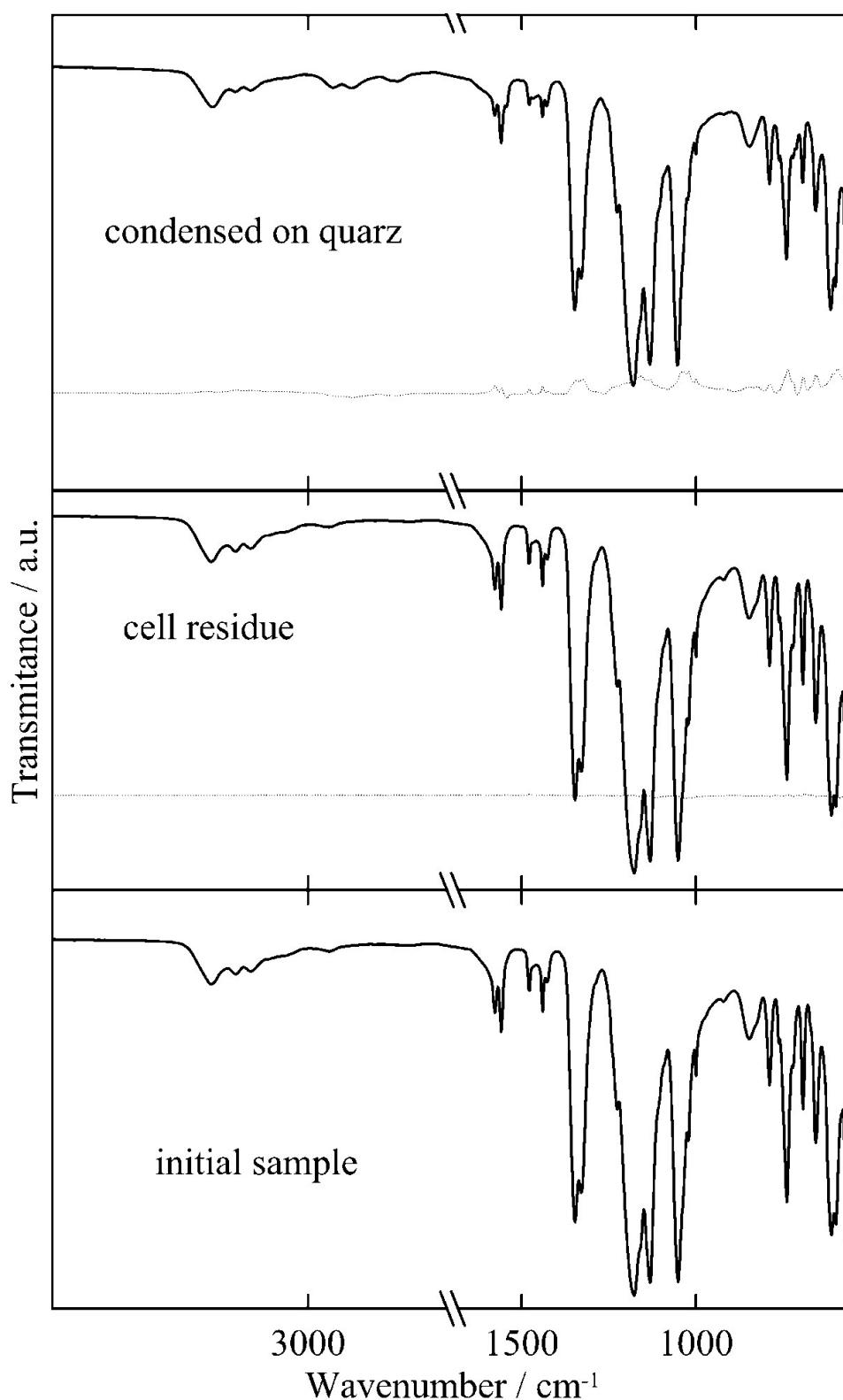|					
1	419.89	163	0.002382	-168.2	126.7
	414.87	105	0.002410	-171.9	127.0
	409.86	67	0.002440	-175.6	127.3
	404.90	43	0.002470	-179.3	127.6
	399.92	27	0.002501	-183.3	128.0
	394.99	17	0.002532	-187.2	128.3
	390.04	10	0.002564	-191.4	128.6
	385.07	6.1	0.002597	-195.6	128.9
	380.09	3.5	0.002631	-200.1	129.3
	375.10	2.1	0.002666	-204.5	129.6
2	422.39	210	0.002367	-166.1	126.5
	417.38	136	0.002396	-169.7	126.8
	412.40	88	0.002425	-173.4	127.1
	407.44	56	0.002454	-177.1	127.5
	402.49	36	0.002485	-180.9	127.8
	397.54	22	0.002515	-184.7	128.1
	392.59	14	0.002547	-188.8	128.5
	387.61	8.2	0.002580	-193.1	128.8
	382.62	4.8	0.002614	-197.6	129.1
	377.65	2.7	0.002648	-202.2	129.4

Figure S44. Infrared spectra for IL **2-NTf₂** during the vapor pressure determination with QCM – Langmuir method. (Dotted line corresponds to the difference between presented spectrum and spectrum of the initial sample). All deviations in spectra stems from small amount of sample condensed at the surface of QCM.
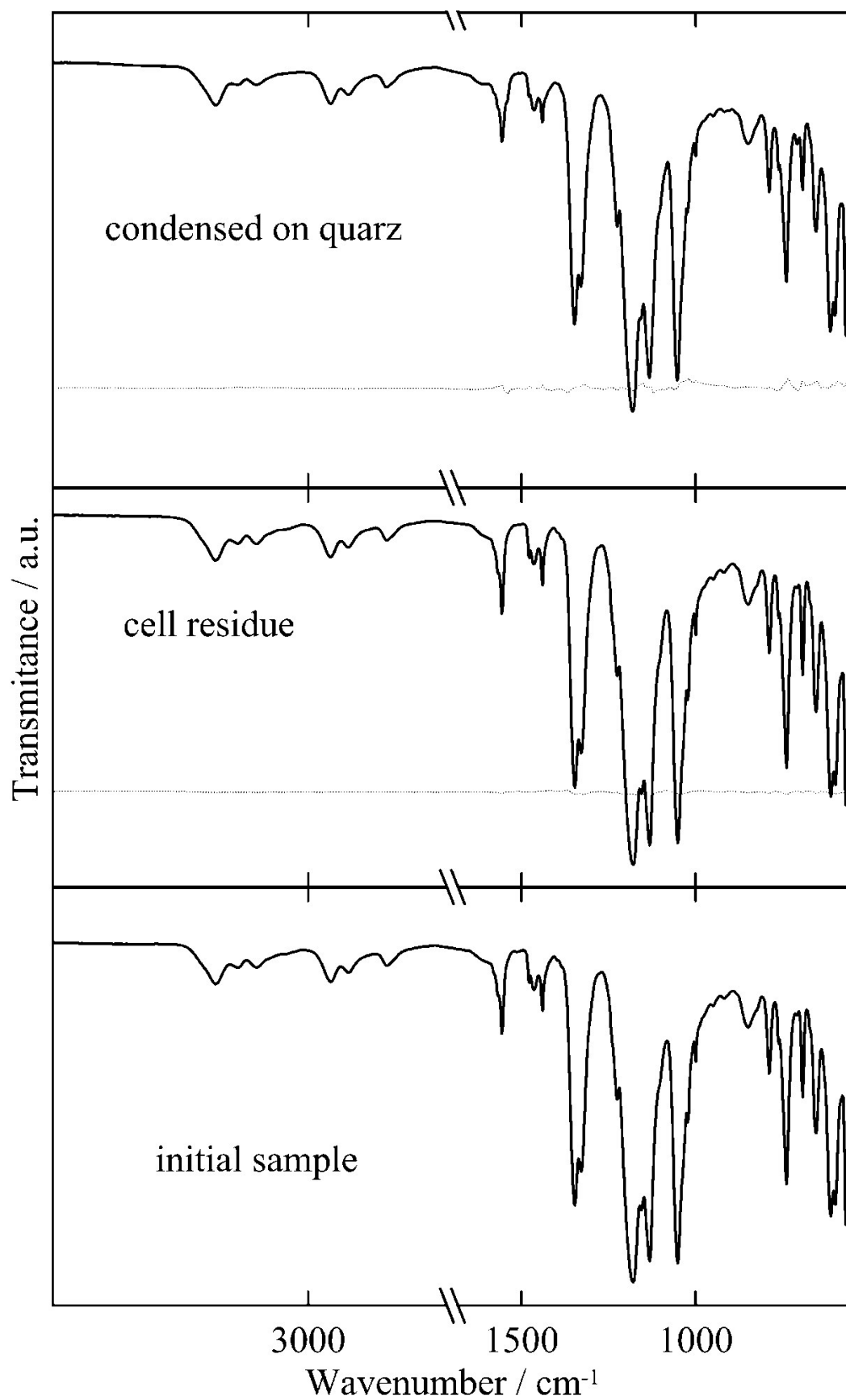
Figure S45. Infrared spectra of IL **3-NTf₂** during vapor pressure determination with QCM – Langmuir method (Dotted line corresponds to the difference between presented spectrum and spectrum of the initial sample).
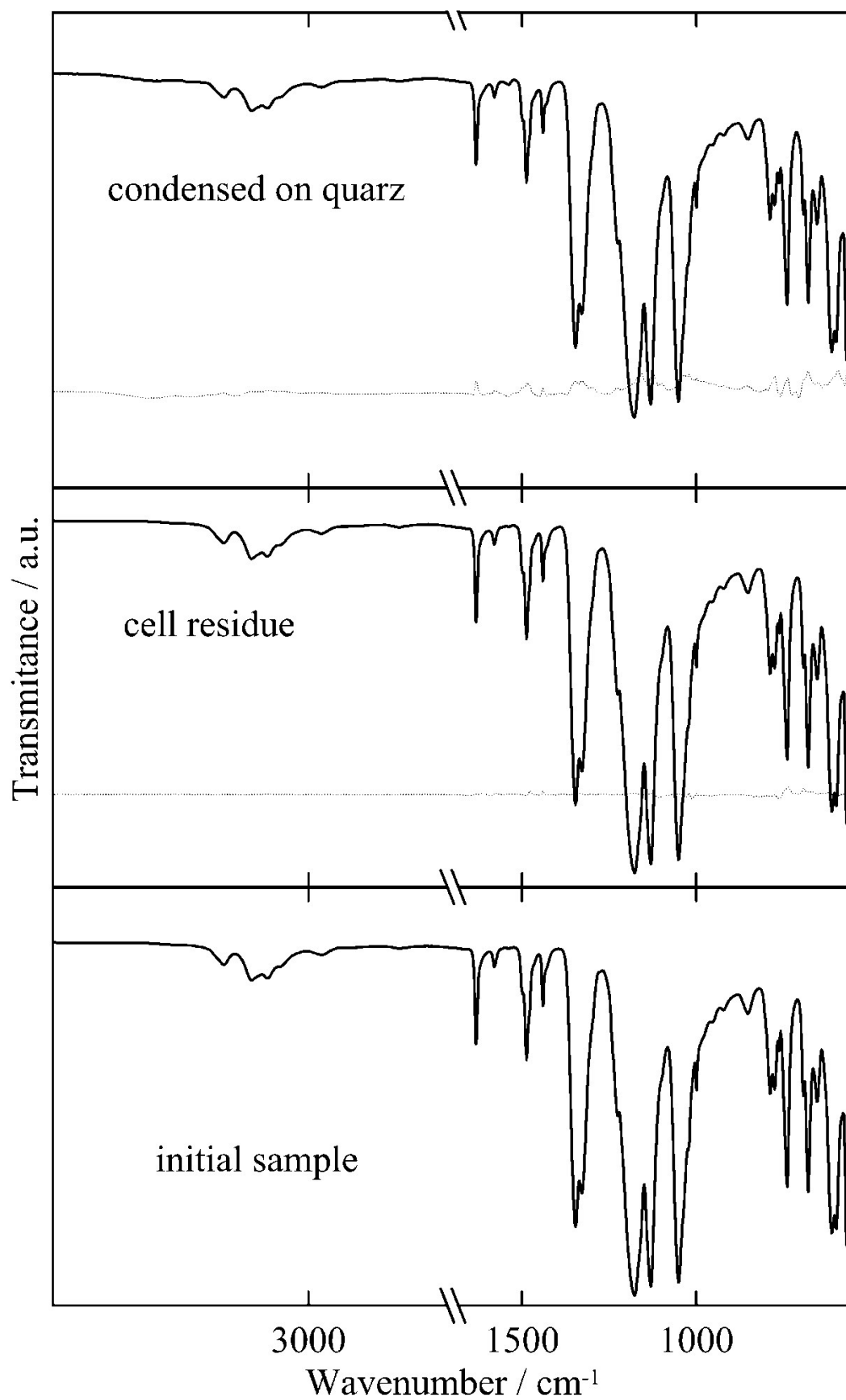
Figure S46. Infrared spectra for **1-NTf₂** during the vapor pressure determination with QCM – Langmuir method (Dotted line corresponds to the difference between presented spectrum and spectrum of the initial sample).

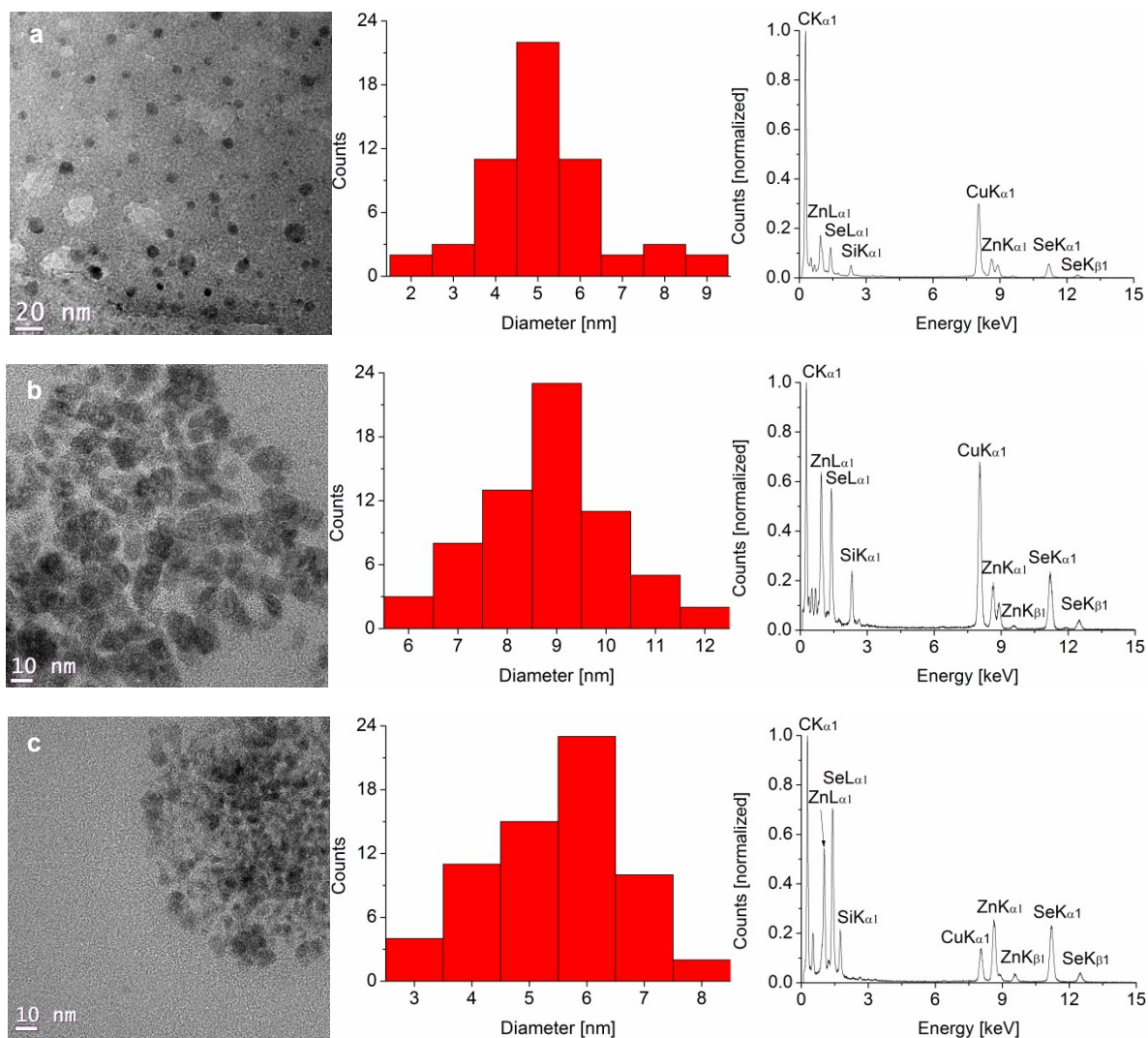## III   Nanoparticle synthesis

Method A

Figure S47. TEM-images, diameter distribution and EDX-Spectra of ZnSe nanoparticles obtained from **method A** from the decomposition of zinc acetate dehydrate in the functionalized ionic liquids (**1-NTf₂** (a), **2-NTf₂** (b) or **3-NTf₂** (c))
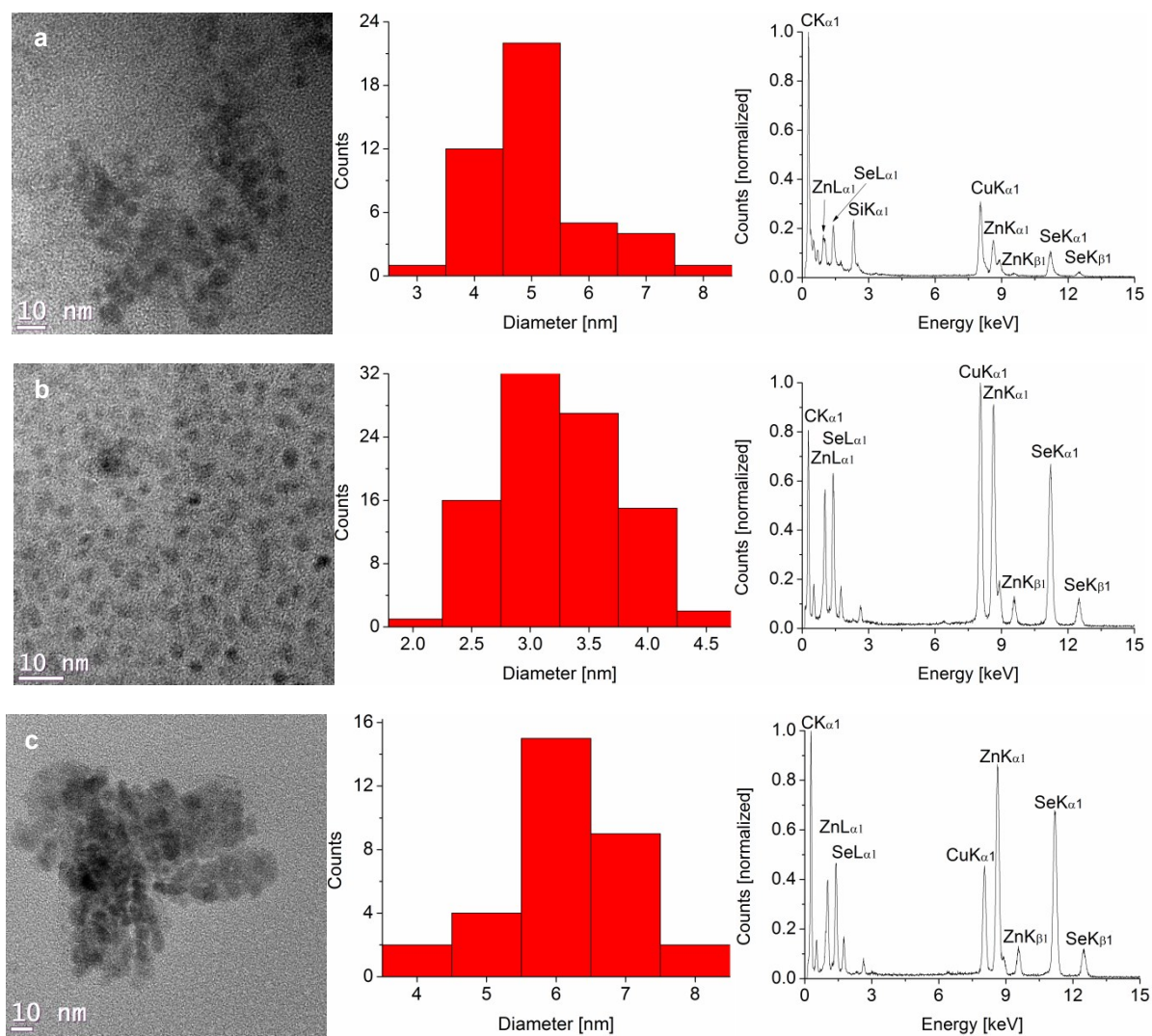
Method B

Figure S48. TEM-images, diameter distribution and EDX-Spectra of ZnSe nanoparticles obtained from **method B** from decomposition of zinc acetate dehydrate and the functionalized ionic liquids (**1-NTf₂** (a), **2-NTf₂** (b) or **3-NTf₂** (c)) in [BMIm][NTf₂]

1   (a) H. D. Flack, M. Sadki, A. L. Thompson, D. J. Watkin, Acta Cryst., Sect. A, 2011, 67, 21–34. (b) H. D. Flack, G. Bernardinelli, Chirality 2008, 20, 681–690. (c) H. D. Flack, G. Bernardinelli, G., Acta Cryst., Sect. A, 1999, 55, 908–915. (d) H. D. Flack, Acta Cryst., Sect. A, 1983, 39, 876–881.

2   X.-J. Yang, F. Drepper, B. Wu, W.-H. Sun, W. Haehnel and C. Janiak, *Dalton Trans.*, 2005, 256-267 and Supplementary Material therein; C. Janiak, *J. Chem. Soc., Dalton Trans.*, 2000, 3885-3896.

3   (a) V. Lozan, P.-G. Lassahn, C. Zhang, B. Wu, C. Janiak, G. Rheinwald, H. Lang, Z. Naturforsch. B, 2003, 58, 1152–1164. (b) C. Zhang, C. Janiak, Z. Anorg. Allg. Chem., 2001, 627, 1972–1975. (c) C. Zhang, C. Janiak, J. Chem. Crystallogr. 2001, 31, 29–35. (d) H.-P. Wu, C. Janiak, G. Rheinwald, H. Lang, J. Chem. Soc. Dalton Trans. 1999, 183–190. (e) C. Janiak, L. Uehlin, H.-P. Wu, P. Klüfers, H. Piotrowski, T. G. Scharmann, J. Chem. Soc., Dalton Trans., 1999, 3121–3131. (f) H.-P. Wu, C. Janiak, L. Uehlin, P. Klüfers, P. Mayer, Chem. Commun., 1998, 2637–2638.

4   CrystalExplorer17, Version 17.5; Turner, M. J.; McKinnon, J. J.; Wolff, S. K.; Grimwood, D. J.; Spackman, P. R.; Jayatilaka, D.; Spackman, M. A. © 2005-217 University of Western Australia, 2017. http://hirshfeldsurface.net

5   (a) J. J. McKinnon, M. A. Spackman, A. S. Mitchell, Acta Cryst., 2004, B60, 627-668. (b) M. A. Spackman, J. J. McKinnon, CrystEngComm, 2002, 4, 378–392. (c) J. J. McKinnon, D. Jayatilaka, M. A. Spackman, Chem. Commun., 2007, 3814–3816.

6   D. H. Zaitsau, M. Kaliner, S. Lerch, T. Strassner, V.N. Emel'yanenko, S. P. Verevkin, Z. Anorg. Allg. Chem., 2017, 643, 114–119.

7   D. H. Zaitsau, A. V Yermalayeu, V. N. Emel'yanenko, S.P. Verevkin, U. Welz-Biermann, T. Schubert, V. N. Emel'yanenko, S. P. Verevkin, U. Welz-Biermann, T. Schubert, Sci. China Chem., 2012, 55, 1525–1531.